Journal of Terramechanics 111 (2024) 41–64

Contents lists available at ScienceDirect

Journal of Terramechanics

journal homepage: www.elsevier.com/locate/jterra

A review of soil modeling for numerical simulations of soil-tire/agricultural tools interaction

Dhruvin Jasoliya [a,*], Alexandrina Untaroiu [a], Costin Untaroiu [a,b]

[a] Department of Mechanical Engineering, Virginia Tech, Blacksburg, VA, USA
[b] Department of Biomedical Engineering and Mechanics, Virginia Tech, Blacksburg, VA, USA

ARTICLE INFO

Article history:
Received 15 June 2023
Accepted 19 September 2023
Available online 13 October 2023

Keywords:
Soil-tire interaction
Soil-tool interaction
Soil classification
Soil testing
Soil constitutive material models
Finite element modeling
Arbitrary Lagrangian Eulerian
Smoothed particle hydrodynamics
Discrete element method

ABSTRACT

The study of deformable soils is one of the key factors in determining the tire, vehicle and/or agricultural tool design parameters. This literature review provides a brief overview of soil classification, soil testing, soil constitutive models, and numerical approaches utilized to model soil-tire/tool interaction. In the past, empirical, semi-empirical, and analytical soil models were used in these studies. However, some limitations occurred in terms of characterization of soil-tire/tool interaction in detail due to a large number of variables such as cohesion, moisture content, etc. In the last few decades, the finite element (FE) method was used with different formulations such as Lagrangian, Eulerian, and Arbitrary Lagrangian Eulerian to simulate the soil-tire/tool interaction. Recently, particle-based methods based on continuum mechanics and discrete mechanics started to be employed and showed good capability in terms of modeling of soil deformation and separation. Overall, this literature review provides simulation researchers insights into soil interaction modeling with tires and agricultural tools.

Contents

1. Introduction . . . 43
2. Soil classification, properties, and testing . . . 43
 2.1. Soil classification . . . 43
 2.2. Soil properties . . . 43
  2.2.1. Physical properties of soil . . . 43
  2.2.2. Mechanical properties . . . 43
 2.3. Soil testing . . . 47
  2.3.1. Laboratory testing . . . 47
  2.3.2. In-Situ testing . . . 47
3. Constitutive models for soil . . . 50
 3.1. Elastic constitutive models . . . 51
 3.2. Elastic-plastic constitutive models . . . 51
  3.2.1. Yield function . . . 51
  3.2.2. Flow rule . . . 53
  3.2.3. Hardening/Softening law . . . 54
 3.3. Elastic-plastic constitutive models for unsaturated soils . . . 54
 3.4. Elastic-visco-plastic constitutive models . . . 55
4. Soil-Tire/Tool interaction studies . . . 55
 4.1. Empirical methods . . . 55
 4.2. Semi-empirical and analytical methods . . . 55
  4.2.1. Soil-tire interaction models . . . 56
  4.2.2. Soil-tool interaction models . . . 56

* Corresponding author.
E-mail addresses: dhruvinj@vt.edu (D. Jasoliya), alexu@vt.edu (A. Untaroiu), costin@vt.edu (C. Untaroiu).

https://doi.org/10.1016/j.jterra.2023.09.003
0022-4898/

Nomenclature

V	Total volume of soil [m^3]	V_s	Soil solid particle volume [m^3]
V_v	Total volume of voids [m^3]	σ	Total stress [MPa]
e	Void ratio	u_w	Pore water pressure [kPa]
S	Degree of Saturation	u_a	Pore air pressure [kPa]
V_a	Air volume [m^3]	σ_n	Net normal stress [MPa]
V_w	Water volume [m^3]	s_{r1}	Matric suction at full saturation [kPa]
σ_c'	Preconsolidation stress [MPa]	s_{r2}	Matric suction at residual state [kPa]
σ'	Present effective stress [MPa]	α_1	Flow parameter
OCR	Overconsolidation ratio	E_t	Tangent modulus [MPa]
Cc	Compression index	E_s	Secant modulus [MPa]
Cs	Swelling index	E_o	Initial modulus [MPa]
s	Matric suction [kPa]	E_{un}	Unload-reload modulus [MPa]
τ_f	Shear strength [MPa]	CI	Cone index [MPa]
c	cohesion [kPa]	W	Applied force [N]
ϕ	Internal friction angle [deg]	r	Base radius of circular cone [mm]
c'	Effective cohesion [kPa]	σ_1	major principal stress [MPa]
ϕ'	Effective internal friction angle [deg]	σ_3	minor principal stress [MPa]
χ	Material parameter	ε	Axial strain
c''	Apparent cohesion [kPa]	a	Material constant
ϕ^b	Internal friction angle based on saturation level [deg]	b	Material constant
s_f	Matric suction at failure [kPa]	F	Yield Function
s_e	Matric suction at air entry [kPa]	P_a	Hardening parameter
k_1	Fitting parameter	ε_{vol}	Volumetric strain
k	Hardening parameter	p'	Mean effective stress [MPa]
ε^p	Plastic strain	p_c'	Preconsolidation stress [MPa]
G	Plastic potential function	M	Critical stress ratio
λ_1	Plastic multiplier	η	Normal stress ratio
θ	Lode angle [deg]	λ	Compression index
J_2	Second Invartiant of deviatoric stress [MPa]	κ	Swelling index
I_1	First invariant of stress tensor [MPa]	$\dot{\varepsilon}$	Strain rate[s^{-1}]
q	Deviatoric stress [MPa]	$\dot{\varepsilon}^e$	Elastic strain rate [s^{-1}]
p	Hydrostatic stress [MPa]	$\dot{\varepsilon}^{vp}$	Visco-plastic strain rate [s^{-1}]
α	Material constant	η	viscosity constant of the material
k_2	Material constant	$\phi(F)$	viscous flow function
h	Material constant	ε^{vp}	Viscoplastic strain
t	Deviatoric stress [MPa]	F_D	Drawbar pull force [N]
β	Soil friction angle [deg]	F_T	Thrust force [N]
d	Drucker-Prager cohesion [MPa]	F_R	Resistive force [N]
R	Cap control parameter	R_c	Rolling resistance [N]
P	Pressure [N/m^2]	L	Length of loaded area [mm]
z	Sinkage [mm]	τ	Shear stress [MPa]
b	Geometry dimension [mm]	j	Shear displacement [mm]
k_c	Cohesion constant [$kN/m^{(n+2)}$]	τ_{max}	Estimated Maximum shear strength [MPa]
k_ϕ	Friction angle constant	j_0	Displacement at maximum shear strength [mm]
n	soil parameter	K_1	Empirical constants
k_c'	Cohesion constant	K_2	Empirical constants
k_ϕ'	Friction angle constant [N/m^3]	K	Shear deformation modulus [GPa]
γ_S	Weight density of soil [N/m^3]		

4.3. Finite-element methods . . . 56
4.3.1. Soil-tire interaction studies . . . 57
4.3.2. Soil tool interaction studies . . . 58
4.4. Particle-based methods . . . 58
4.4.1. Smoothed particle hydrodynamics . . . 59
4.4.2. Discrete element method . . . 60
5. Summary . . . 61
Declaration of Competing Interest . . . 61
Acknowledgments . . . 61
References . . . 61

1. Introduction

Performance of agricultural tools and tires is not only dependent on their design parameters but also on the soil conditions. The studies in the field of terramechanics focuses on parameters such as soil compaction, soil cutting forces, fuel efficiency, tractive effort, tire rolling resistance, drawbar pull, and steering effort. The outputs of these studies are highly dependent on the soil properties and determining them is quite complex. Understanding the behavior of the soil and the factors influencing it can be done with the help of geomechanics principles, a science that focuses on the mechanical characterization of soil (He et al., 2019; Wong, 2022).

A wide range of laboratory and in-situ testing methods are available in the field of geomechanics and terramechanics. To determine soil properties accurately, it is important to select the appropriate test based on the soil type, moisture content, strain rate, and constitutive material proposed to be used for modeling. For example, these tests may provide information about the stress–strain relationship, elastic modulus, Poisson ratio, preconsolidation stress, cohesion, and internal friction angle in the context of soil behavior that experiences high plastic deformations (Bekker, 1956; Lade, 2016).

The most appropriate constitutive material model could be selected based on the pertinent output of the soil-tire/tool interaction studies and the available soil testing data. For example, nonlinear elastic material models require two parameters while more sophisticated elastic–plastic material models require additional plasticity parameters (Duncan and Chang, 1970). The number of elastic–plastic material model parameters is also dependent on their formulation. Furthermore, elastic–plastic models can be expanded to elastic-viscoplastic models with additional parameters to model the strain rate effect on the overall behavior of the soil (Perzyna, 1966; Poodt et al., 2003).

In the past, soil-tire/tool interaction studies were done using empirical models, semi-empirical and analytical models which are based on mathematical formulations and provide a good preliminary estimation of performance parameters (Contreras et al., 2013). More detailed and in-depth studies were performed using finite element (FE) methods and particle-based methods. Different formulations are used in the FE method to increase the accuracy of the numerical solutions (Chi and Kushwaha, 1990; Shoop et al., 2005; Xu et al., 2020). Recently, particle-based methods showed a good ability to capture soil discontinuous behavior using either continuum or discrete modeling approaches (Ma et al., 2009; Smith and Peng, 2013; El-Sayegh et al., 2018; Tekeste et al., 2019; Hu et al., 2021).

This literature review provides a brief overview of soil classification, mechanical properties, testing methods, constitutive models, and modeling approaches used in soil-tire/tool studies. Furthermore, the relative advantages and disadvantages of various approaches are also discussed.

2. Soil classification, properties, and testing

Soils form through the physical and chemical weathering of rocks and sediments. The soil particle size and its distribution depend on the weathering conditions. Cohesion between the soil particles, relative density and variation of soil strength based on moisture content affects the overall behavior of the soil. Therefore, to develop accurate numerical models of soil, a detailed study of all these variables is required.

2.1. Soil classification

Soils are mainly categorized based on particle size as coarse-grained soil (gravel and sand) and fine-grained soil (sand and silt) (Fig. 1). Soils are also divided into two subcategories: cohesionless and cohesive. Cohesionless soils have particles that do not adhere to one another . They have high permeability and tend to transmit water easily; the shear strength of such soils is only dependent on the friction between the particles. On the contrary, cohesive soils can retain moisture and exhibit plastic behavior by adhering to each other (Keaton, 2018). Because of the cohesion these soils have high shear strength compared to cohesionless soil and this property is very critical from the soil-tire/tool interaction perspective.

2.2. Soil properties

Extensive studies have been undertaken in the field of geomechanics (Budhu, 2015; Das, 2021) and terramechanics (Bekker, 1956; Wong, 1989; Muro and O'Brien, 2004) for understanding the soil behavior. These studies have concluded that the soil behavior is governed by physical properties (particle size distribution, degree of saturation, density, etc.) and mechanical properties (shear strength, compressibility, and stiffness). Soil properties mentioned in the literature relevant to soil-tire/tool studies and their testing methodology are discussed in the following sections.

2.2.1. Physical properties of soil

Soil is made up of solid, liquid and gas. In most cases, the liquid and gas components are water and air, respectively (Fig. 2). The spaces between the solid particles (called voids) are accumulated by either air, water, or both. The relative proportion of the three phases has a significant effect on the physical properties of the soil.

Total volume of the soil (V), total volume of voids (V_v), void ratio (e) and degree of saturation (S) could be written as (Eq. (1- 4)),

$$V = Va+Vw+Vs \tag{1}$$

$$V_v = V_a + V_w \tag{2}$$

$$e = V_v/V_s \tag{3}$$

$$S = V_w/V_v \tag{4}$$

where V_a is volume occupied by the air, V_w is volume occupied by the water, V_s is volume occupied by the solid soil particles.

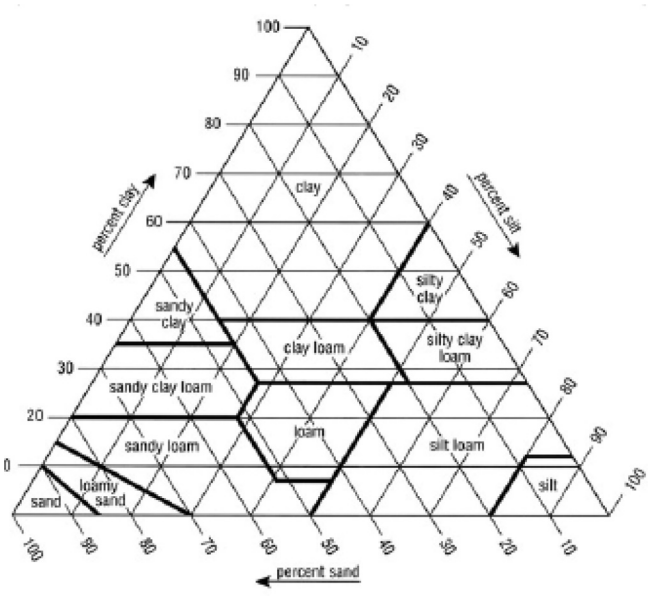

Fig. 1. Soil classification triangle based on relative proportion of sand, clay and silt (NRCS, 1993).

The degree of saturation is an indication of water presence in the voids. For a fully saturated soil (S = 1) all the voids are filled with water (no air). Similarly, for dry soil (S = 0) there is only air in the voids (no water). For unsaturated soils (0 < S < 1), the relationship between the degree of saturation and moisture content of soil is usually represented through the soil water retention curve.

The soil water retention curve (SWCC) is extensively used in studying the variation of soil properties with change in moisture content. A typical SWCC (Fig. 3) is represented by a relationship between the degree of soil saturation/moisture content and matric suction i.e., the difference between the pore air pressure and pore water pressure. Usually, the pore water pressure varies with the groundwater level and pore air pressure varies with the environmental changes which create unsaturated soil conditions. The curve can be divided into three distinct stages- boundary effect stage, transition stage and residual stage. There is a drastic change in the behavior of soil between the air-entry value and residual point which is spanned by a transition zone. The difference between drying and wetting conditions appears as a hysteresis zone; however, drying curves are frequently used for analyzing SWCC (Eyo et al., 2020).

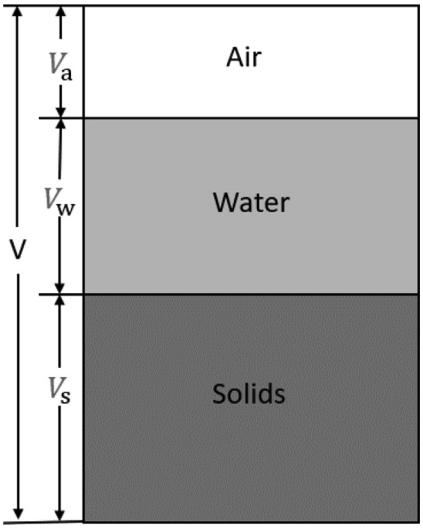

Fig. 2. Composition of Soil. Redrawn from (Helwany, 2007).

As a part of large-scale studies on soil behavior, different testing techniques are used to measure SWCC (Stoltz et al., 2012; Wang et al., 2015; Al-Mahbashi et al., 2020). The measured data points of the SWCC can be fitted with an appropriate mathematical model (Wen et al., 2015). Some of the testing techniques for determining the SWCC could be used in the soil-tire/terrain studies to better understand the impact of soil moisture content.

2.2.2. Mechanical properties of soil

Soil mechanics describes the soil as granular material and investigates various soil mechanical properties (e.g., compression, stiffness, strength, permeability) which affect the stress–strain relationships and yielding function. The study of mechanical behavior of the soil is very different from metals and other similar materials due to the frictional nature of the soil and coupling between the shear and volume change. All the principles of soil mechanics are equally applicable to fine-grained soils (cohesive soils) and coarse-grained soils (cohesionless soils).

As discussed earlier, soil is a multiphase medium with mixture of soil particles, air, and water. The degree of saturation of soil, particle packaging and its stress history have a significant impact on the mechanical properties of the soils. An extensive testing program is required to characterize the soil properties based on all the mentioned parameters which makes soil modeling challenging. In this section, a detailed review of the various mechanical properties and their variations is presented, which can be further used for the study of tire/tool interaction with different types of soils.

2.2.2.1. Compressibility of soil. For soil-tire/tool interaction, it is important to know how the soil volume changes under tire/tool load. This property is called soil compressibility and the process is known as soil compression. Compressibility of soil is studied in terms of volumetric strain and total stress for dry soil. Stresses in saturated soil are calculated in terms of effective stress σ' ($\sigma - u_w$), which is the difference between total stress and pore water pressure, to take into account the fact that pore water trapped in the soil also contributes to volumetric deformation (Terzaghi, 1943). Similarly for unsaturated soils, to include the influence of

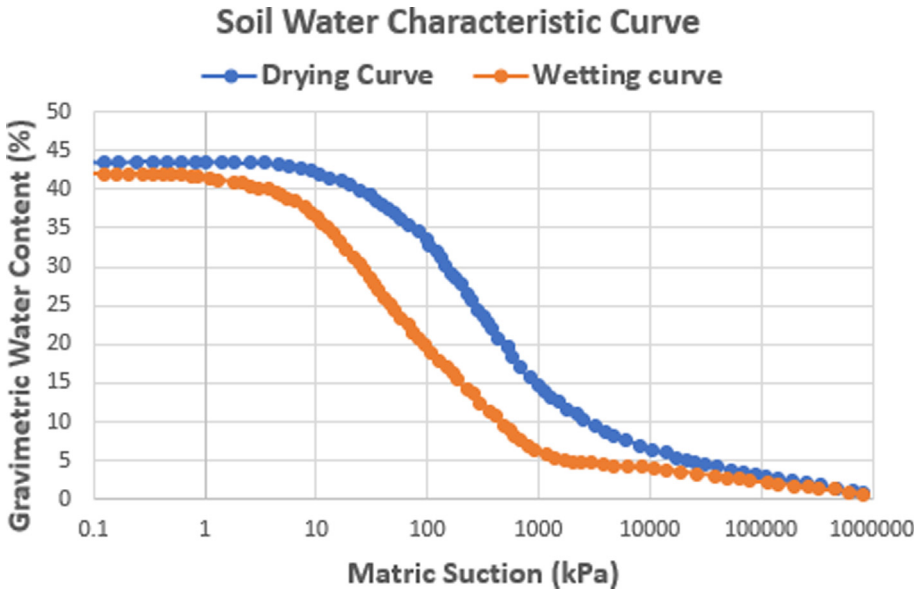

Fig. 3. Typical Features of SWCC. Redrawn from (Eyo et al., 2020).

pore air, stresses are estimated in terms of net normal stress (σ-u_a), which is the difference between total stress and pore air pressure (Ho et al., 1992). Usually, volumetric strain is represented by the void ratio change in soil compressibility studies. Compressibility of soil is affected by the soil particle distribution, particle size and moisture content (Nayyeri Amiri, 2010).

The void ratio (e) changes slowly till it reaches the pre-consolidation stress (maximum stress in soil history) and then there is a rapid change in the void ratio. The plot of e vs log σ' is nonlinear but it is idealized as linear for calculation of pre-consolidation stress (Fig. 4) (Casagrande, 1936). The slope of the loading line is defined as compression index (Cc) and slope of the unloading line is defined as swell index (Cs) of the soil (Terzaghi and Peck, 1948). Based on the present maximum effective stress, soils are classified as *normally consolidated soil* whose present effective stress is same as pre-consolidation stress and *over consolidated soils* whose present effective stress is lower than pre-consolidation stress. Over-consolidation ratio (OCR) defines the extent of over-consolidation of the soil and it is defined as (Eq. (5)) –

$$OCR = \frac{\sigma_c'}{\sigma'} \tag{5}$$

where, σ_c' is pre-consolidation stress of the specimen and σ' is present effective vertical stress.

For saturated soil, only one independent state stress variable, effective stress σ' is required to study the volume change behavior of soil. However, for unsaturated soil, two state stress variables: net normal stress σ_n and suction s (u_a -u_w) are required to understand the volume change behavior (Fredlund and Morgenstern, 1976). Many researchers have attempted to study the volume change behavior of unsaturated soils using suction controlled oedometer tests (Ho et al., 1992; Slatter et al., 2000; Aversa and Nicotera, 2002; Głuchowski et al., 2020). These studies indicate that the swelling index and compression index are dependent on the moisture content and the pre-consolidation stress increases with an increase in moisture content. Therefore, while modeling unsaturated soil for tire/tool interaction, variation in compressibility parameters based on the moisture content should also be taken into account to predict accurate results.

2.2.2.2. Shear strength of soil. The shear strength of the soil depends on confining stress (stress corresponding to the applied normal load), strain rate, drained/undrained loading, density, over-consolidation ratio and direction. Furthermore, the soil strength varies quite significantly based on the water content of the soil. The soil strength concept was developed based on the principles of brittle materials, and it was later modified to account for the presence of moisture content (Vanapalli, 2009).

Material failure was also applied for soils based on values of both normal stress and shear stress (Mohr, 1900). For example, in most soil mechanics problems, the linear relationship (Eq. (6)) between the shear stress and normal stress (as Mohr-Coulomb failure criterion) is considered for calculating the failure envelope (Coulomb, 1776).

$$\tau_f = c + \sigma tan\phi \tag{6}$$

where, c is cohesion, ϕ is internal friction angle, σ is normal stress on the failure plane and τ_f is the shear strength. For fully saturated soil, the Mohr-Coulomb (MC) criterion is expressed in terms of effective parameters as shown in (Eq. (7)).

$$\tau_f = c' + \sigma' tan\phi' \tag{7}$$

where, c' and ϕ' are cohesion and internal friction angle based on effective stresses. A typical Mohr-circle and its corresponding failure envelope based on the testing data of saturated soil (Fig. 5).

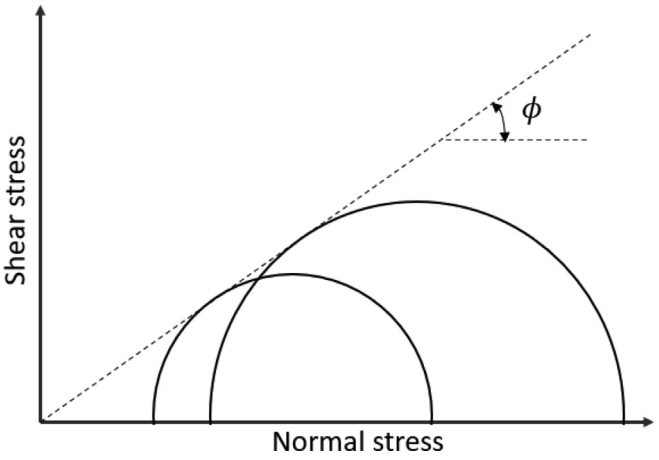

Fig. 5. Mohr circle and failure envelope for saturated soil. Redrawn from (Banerjee, 2017).

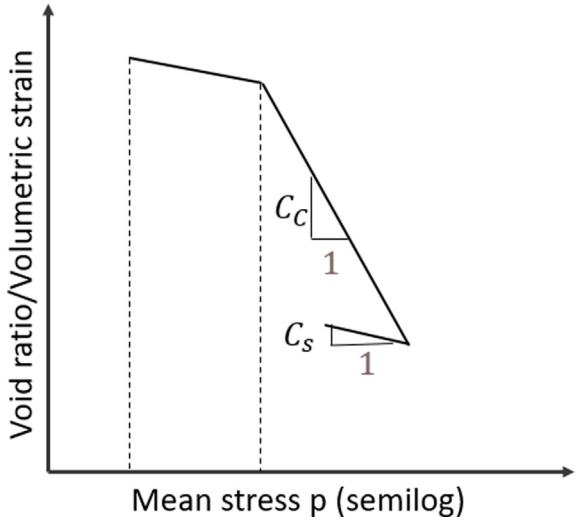

Fig. 4. Typical Soil compression curve with linear approximation for preconsolidation stress estimation. Redrawn from (Helwany, 2007).

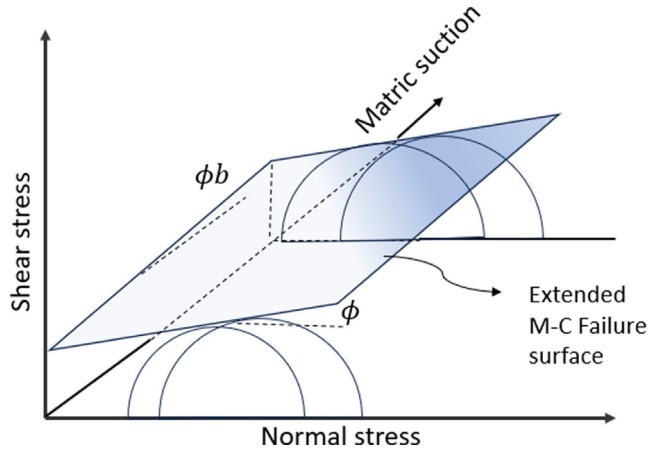

Fig. 6. Failure envelope for unsaturated soil. Redrawn from (Fredlund and Morgenstern, 1977).

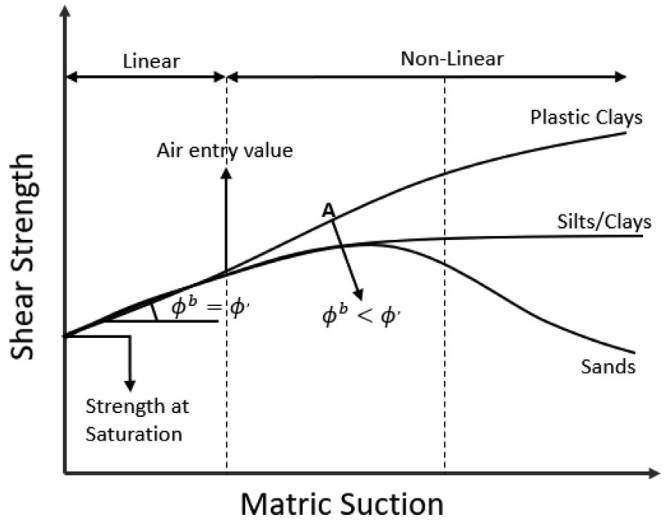

Fig. 7. Shear Strength variation with suction (Saturation level) for different soils. Redrawn from (Vanapalli, 2009).

The shear strength of unsaturated soils is calculated by extending the conventional MC-criterion for saturated soils using two state parameters- net normal pressure σ_n (f(σ,u_a)) and matric suction s (u_a -u_w) and one degree of saturation dependent material parameter χ (Bishop, 1959).

$$\tau_f = c' + (\sigma - u_a)tan\phi' + (u_a - u_w)[\chi tan\phi'] \quad (8)$$

$$c'' = c' + (u_a - u_w)[\chi tan\phi'] \quad (9)$$

The value of material parameter χ varies between 0 and 1, where 0 represents the dry conditions and one represents the fully saturated soil, essentially converting extended MC criterion into conventional MC criterion. c'' is apparent cohesion which changes with suction while the friction angle ϕ' associated with net normal stress remains constant which indicates it is dependent just on particle interaction and not on water content present (Eq. (9)). Hence, an important aspect of modeling unsaturated soil is to understand the change in apparent cohesion with suction which is highly dependent on the type, particle size distribution and soil water characteristic curve of the soil.

Later, another equation based on two independent state variables i.e., net stress and suction based on MC criterion (Fig. 6) was proposed to calculate the shear strength of the unsaturated soil (Fredlund and Morgenstern, 1977).

Table 1
Shear strength relations for unsaturated soils.

Contribution	Shear Strength Parameter estimation ($\chi / \frac{tan\phi_b}{tan\phi'}$)
(Russell and Khalili, 2006)	1 for $(s/s_e) \leqslant 1$ $(s/s_e)^{-0.55}$ for $(s/s_e) \leqslant 25$ $25^{0.45}(s/s_e)^{-1}$ for $(s/s_e) \geqslant 25$
(Khalili and Khabbaz, 1998)	$\left\{\frac{s_f}{s_e}\right\}^{-0.55}$
(Öberg and Sällfors, 1997)	S
(Vanapalli et al., 1996)	$(S)^{k_1}$
(Toll and Ong, 2003)	$\left(\frac{s-s_{r2}}{s_{r1}-s_{r2}}\right)^{k_1}$
(Alonso et al., 1990)	α_1
(DE'AN et al., 2000)	$\left(\frac{k_1}{S+k_1}\right)$

where s- matric suction, s_f-matric suction at failure, s_e- matric suction at air entry, S- degree of saturation, k_1-fitting parameter, s_{r1}- matric suction at full saturation, s_{r2} -matric suction at residual state, α_1- flow parameter.

$$\tau_f = c' + (\sigma - u_a)tan\phi' + (u_a - u_w)tan\phi^b \quad (10)$$

where, ϕ^b is a friction angle that describes the change of shear strength relative to matric suction. The value of suction up to which shear strength and total stress increases at the same rate is known as air entry value (Fig. 7) (Fredlund and Rahardjo, 1993). The material parameter χ is defined as the ratio between friction angle representing the degree of saturation and intrinsic friction angle of soil (Eq. (11)).

$$\chi = \frac{tan\phi_b}{tan\phi'} \quad (11)$$

Above mentioned relations (Eq. (8) & Eq. (10)) are widely used for the shear strength interpretation and modeling of unsaturated soils. Several authors (Table 1) have modified these equations using exponential, hyperbolic, soil water characteristic curve dependent, critical state soil mechanics based relations using experimental data.

2.2.2.3. Soil stiffness. The soil usually shows a non-linear stiffness which depends on the soil type, density, over-consolidation ratio and direction. The soil non-linear stress–strain behavior can be approximated using four moduli (Fig. 8) (E_t-tangent modulus, E_s-Secant modulus, E_o-initial modulus, and E_{un}-Unload-reload modulus). As strain increases, soil stiffness rapidly decreases (Fig. 9). Hence, soil stiffness has little effect on the general behavior of soil in large deformation investigations like soil-tire/tool simulations (Atkinson, 2000).

For unsaturated soils, volumetric water content and matric suction have strong influence on the soil stiffness as concluded through experimental studies (Ng et al., 2009; Sawangsuriya et al., 2009)(Fig. 10). There are empirical and power law functions that provides the relationship between suction and stiffness moduli, a typical trend observed is with an increase in suction, soil stiffness increases (Oh et al., 2009). These functions can be used to update the value of stiffness based on the suction value for soil constitutive models used in soil-tire/tool studies.

Numerical studies involving large deformations, such as soil-tire/tool interactions, tend to usually ignore the contribution of the elastic strain compared to plastic strains (Shoop et al., 2005). Models which are based on elastic–plastic framework, the unload-reload Young's modulus value is directly used for defining the elastic behavior of the soil (Chauhan et al., 2019).

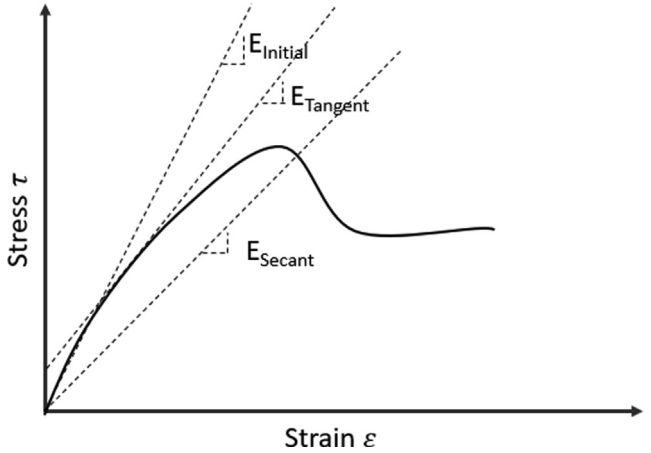

Fig. 8. Nonlinear stress strain behavior of dense sandy soil. Redrawn from (Eslami et al., 2019).

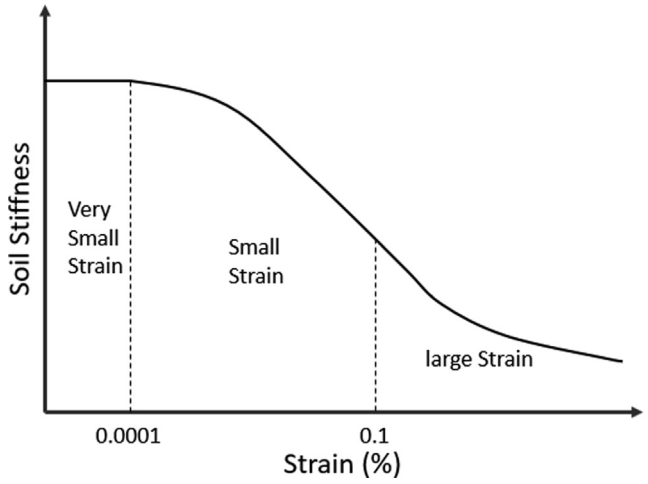

Fig. 9. Stiffness degradation with strain. Redrawn from (Likitlersuang et al., 2013).

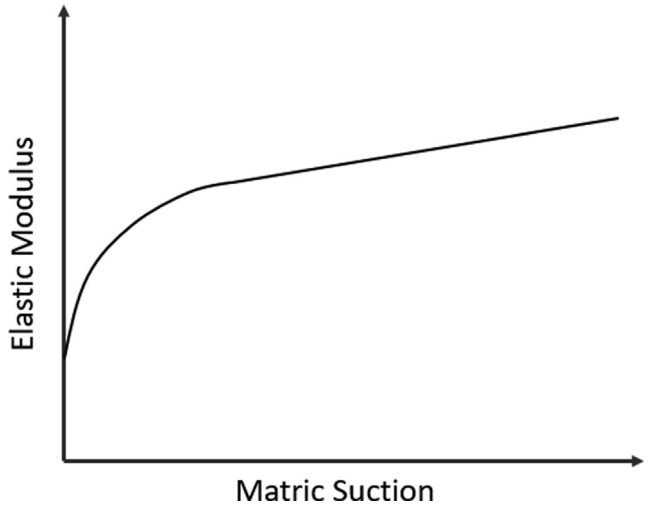

Fig. 10. Variation of Young's modulus with matric suction. Redrawn from (Han and Vanapalli, 2016).

2.3. Soil testing

For numerical simulation of soil, accurate estimation of physical and mechanical properties is very critical. Soil behavior is dependent on a large number of variables (e.g., cohesion, internal friction angle, degree of saturation, density, stress paths, compression index, etc.), hence selection of the proper testing method itself is very important. The selected method should produce the results as close as possible to the field values and provide all the data necessary for the numerical simulation. Usually, based on the complexity and desired output of the simulation, data from either laboratory test or in-situ test is used. Both approaches have their own advantages and disadvantages which are discussed in detail in later sections along with the most common types of soil tests and their data interpretation.

2.3.1. Laboratory testing of soil

The main aim of soil testing is to measure the soil response for a given load, displacement, and environmental conditions. The laboratory testing has the ability to accurately control and measure soil response which makes it very useful for deriving the constitutive model parameters for a given soil. The main drawback of laboratory testing is the complexity of obtaining undisturbed soil samples. However, laboratory techniques, such as direct shear test and triaxial test, are still used extensively for the mechanical characterization of soil (Potts et al., 2001). Parameters obtained through these tests are directly or indirectly used to calibrate the soil constitutive models used in the numerical modeling of soil-tire/tool interaction.

2.3.1.1. Direct shear test. The direct shear test (Fig. 11) is the simplest test available to calculate the shear strength of the soil. For a given normal load, incremental shear force is applied, and shear displacement is measured in the horizontal direction. Further, the vertical height of the specimen is measured to calculate the compression and dilation of the sample.

The behavior of loose sand and normally consolidated (NC) clay is similar for the direct shear test. With the increase in shear strain (Fig. 12-a), shear stress increases gradually till it reaches a constant shear stress value also known as critical shear stress. Such soils usually compress in vertical direction with an increase in shear strain. For, dense sands and over-consolidated (OC) clays, shear stress value reaches the peak value (used to calculate failure envelope) with an increase in the shear strain before settling down to the critical stress value (Fig. 12-a) (Helwany, 2007).

With increase in shear strain in dilative soils, the height of the sample increases (Fig. 12-b). Hence, an appropriate constitutive material model has to be selected for modeling dilative soils which can handle strain softening behavior under large shear strains.

For performing the direct shear test of unsaturated soils, the conventional apparatus has to be modified to control the suction which directly controls the degree of saturation of the soils (Escario and Saez, 1987; Gan et al., 1988; Huat et al., 2005). The soil strength varies with change in suction (Fig. 13). The non-linear failure envelope obtained can be fitted with an appropriate model to predict the soil strength and can be used further for numerical simulation of the unsaturated soils.

Using the direct shear test method, shear strength of saturated and unsaturated soils can be determined easily compared to the extended test like triaxial test. There are two major drawbacks of direct shear testing, 1) undrained shear strength of the soil only be estimated if the shearing rate is fast as it doesn't have any control mechanism to stop the drainage and 2) the sample is forced to fail along the shearing plane instead of its weakest plane which might lead to inaccurate results. However, direct shear test method is a quick way to characterize the basic soil behavior. (e.g. dilatancy, shear strength variation with suction, etc.) (Nam et al., 2011).

2.3.1.2. Triaxial test. Triaxial testing is used extensively for determining the shear strength parameters of the soil. The cylindrical soil specimen is then subjected to predetermined confining pressures (consolidation step) and shearing stress for given drainage conditions (Fig. 14). Deviator load, vertical deformation, volume change or pore water pressure are obtained as output from the test. Based on the various drainage conditions, triaxial tests are classi-

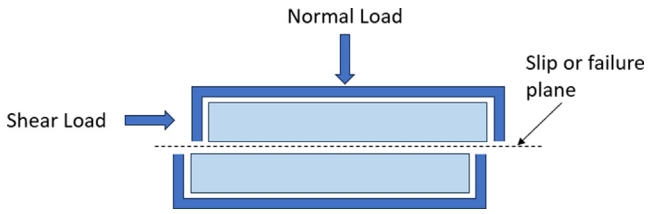

Fig. 11. Direct shear test apparatus. Redrawn from (Budhu, 2015).

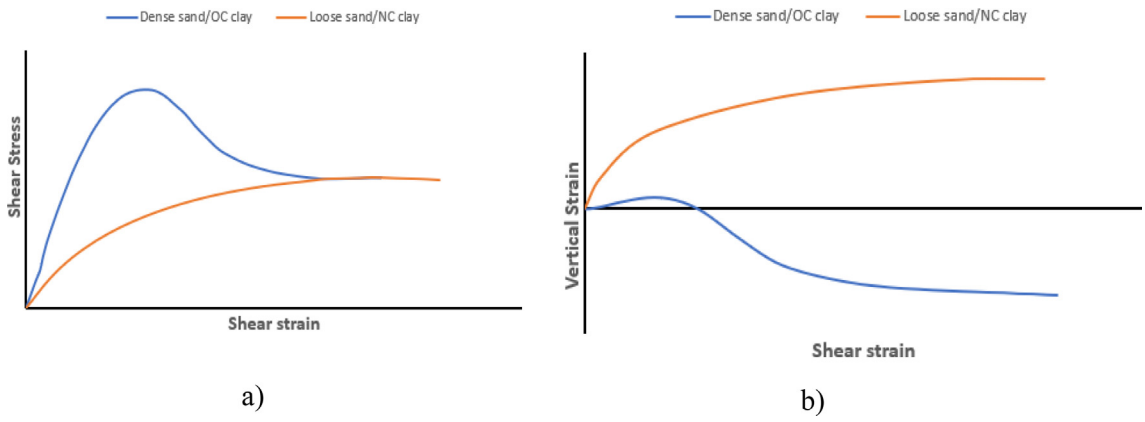

Fig. 12. Typical direct shear test results for different types of clays and sands. (a) Variation of shear stress with shear strain (b) Variation of vertical strain with shear strain. Redrawn from (Budhu, 2015).

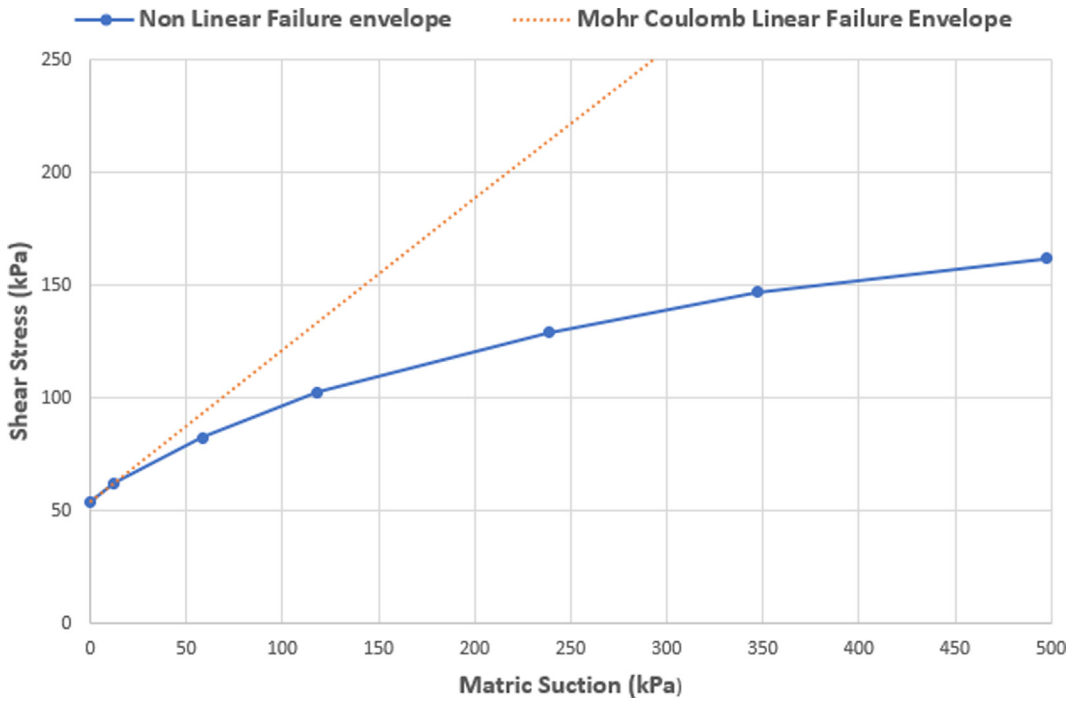

Fig. 13. Nonlinear Failure envelope of Glacial till. Redrawn from (Gan et al., 1988).

fied into three types of tests, consolidated drained test (CD), consolidated undrained test (CU) and unconsolidated undrained test (UU). Appropriate test selection should be done based on the closest field conditions for which soil strength needs to be determined (Lade, 2016).

CD test is usually performed for coarse-grained soil and long-term loading of fine-grained soil. The test is conducted at a slow rate such that there is no pore water-pressure change as water is allowed to drain. The void ratio, dry density, and volume of the specimen changes at the end of the test (Fig. 15). CU test is performed for characterizing the short-term behavior of fine-grained soils under the load. As water is not allowed to drain during the test, the soil specimen volume remains same, but the pore water pressure increases with the increase in axial strain, and it is measured throughout the test (Fig. 16). For UU test, the water is not allowed to drain during consolidation step also contrary to CU test. The change in pore water pressure is not measured during the test (Fig. 17). For the testing of unsaturated soils usually it is very difficult to control the suction conditions and measure pore water and pore air pressure. Hence, CU and CD test are used for the testing of saturated soils and UU test is preferred for the testing of unsaturated soils.

For the development of constitutive framework of unsaturated soils using UU test data, several testing studies based on effective stress approach (Escario and Saez, 1987; Kohgo et al., 1993; Toll and Ong, 2003) and two independent state variable approach (Fredlund and Morgenstern, 1977; Fredlund et al., 1987; Drumright, 1989; Toll, 1990) have been undertaken. Because of the complexity of two state variable approach, currently effective stress approach is used extensively for modeling of unsaturated soils using UU triaxial test data (Khalili et al., 2004). Further, experimental interpretation of UU test data based on total stress approach is also used in soil modeling (Shoop et al., 2005; Huang et al., 2022). Total stress approach doesn't require pore water and pore air pressure measurement, which is quite difficult to control and measure. Also, soil parameters obtained through total

Fig. 14. Triaxial test equipment setup (Geotechnical Lab, Virginia Tech).

stress approach can be directly used with single phase soil constitutive material models already available in commercial FE software.

Triaxial testing has several advantages over direct shear test, the soil sample is allowed to fail along the weakest plane, further control over drainage and measurement of pore water pressure can accurately predict the soil strength parameters ,especially for the undrained conditions. Testing over several different stress paths can be done over several different shearing rates. One of the major drawbacks of triaxial testing is it is quite time consuming, especially for CU and CD test and further, the sample disturbance might affect the overall results. Still, triaxial test data is very critical for the development of the elastic–plastic and elastic-visco-plastic material models required for the numerical simulations of the soil.

2.3.2. In-Situ testing of soil

In-situ testing of the soil is extensively used in the field of terramechanics for characterization of the soil properties (Janosi and Command, 1959; Wong, 1989; Wong, 2022). In-situ testing methods are preferred over laboratory testing because of lab sample disturbance, large volume of the soil can be tested, quickly and cost effectively. Characterization of soil is solely based on the uncertain empirical correlation of in-situ test data and soil properties, further specific behavior of the soil for given loading condition cannot be predicted using in-situ testing methods are few of the disadvantages. Cone penetration test (CPT), bevameter test, Standard penetration test (SPT), Vane shear test are some of the in-situ testing methods used to study the volume change behavior and soil strength extensively (Mitchell et al., 1978). Out of all in-situ methods described in the literature, CPT is the most common test used

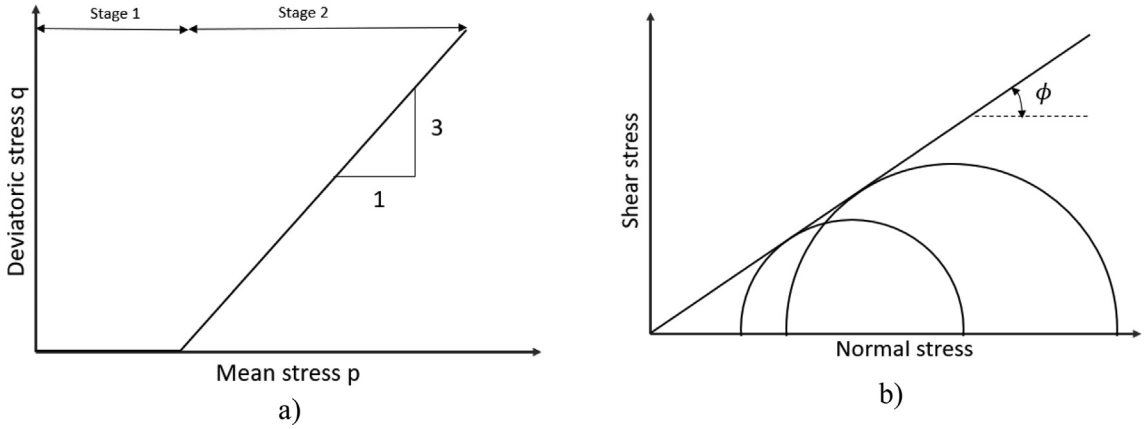

Fig. 15. a) Stress path and b) mohr circle diagram for cd triaxial test. Redrawn from (Das, 2021).

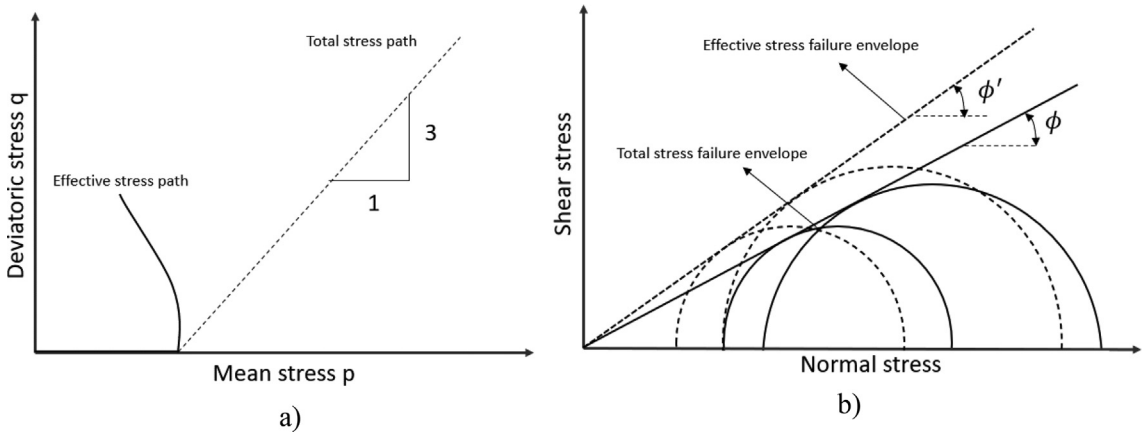

Fig. 16. a) Stress path and b) mohr circle diagram for cu triaxial test. Redrawn from (Das, 2021).

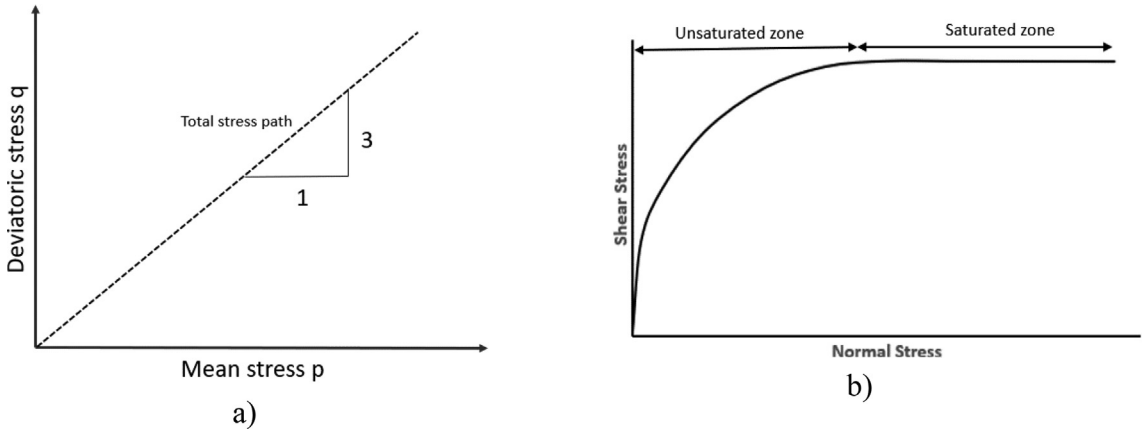

Fig. 17. a) Stress path and b) mohr circle diagram for uu triaxial test. Redrawn from (Das, 2021).

in soil characterization for soil-tire/tool studies which is reviewed in more detail in the next part of this section.

2.3.2.1. Cone penetration test (CPT). The cone penetration technique was developed to characterize soil on a go-no-go basis for vehicle mobility. Cone penetrometer has a 30-degree cone at the base with 0.5 in^2 of area (Fig. 18). It also consists of a dial which indicates the force required to penetrate the ground. Cone index indicates the soil resistance against the penetration, and it is calculated as (Eq. (12))-

$$CI = W/\pi r^2 \tag{12}$$

where, CI = cone index, W = force applied and r = base radius of circular cone.

Soil properties such as cohesion, internal friction angle, compression index and internal friction angle are usually derived using CPT data through empirical relations (Wang et al., 2017). These empirical relations requires detailed test data for calibration. Hence, physics based relations between soil properties and cone index were developed based on cavity expansion theory (Rohani and Baladi, 1981). Solutions of these physics-based nonlinear equations are quite complex and numerical techniques are preferred over analytical solutions.

One of the important aspects of soil characterization is the variation of mechanical properties with change in moisture content (Fig. 19). Past studies, indicate that the cone index is less sensitive to the change of compression and shear strength of the soil with an increase in the moisture content (Mulqueen et al., 1977). Empirical relations developed for saturated and dry soil to calculate the internal friction angle and density tend to overpredict the values for the unsaturated soils (Pournaghiazar et al., 2013). Hence, to determine the mechanical properties of the soil with variable moisture content, material optimization tools or combination of in-situ and laboratory test data are used in order to overcome the limitations of both empirical relations and physics based models (Jarast and Ghayoomi, 2018).

3. Constitutive models for soil

The modeling of soil is very challenging due to its non-linear, time dependent, plastic, and anisotropic properties. Based on the required accuracy of modeling and test data availability an appro-

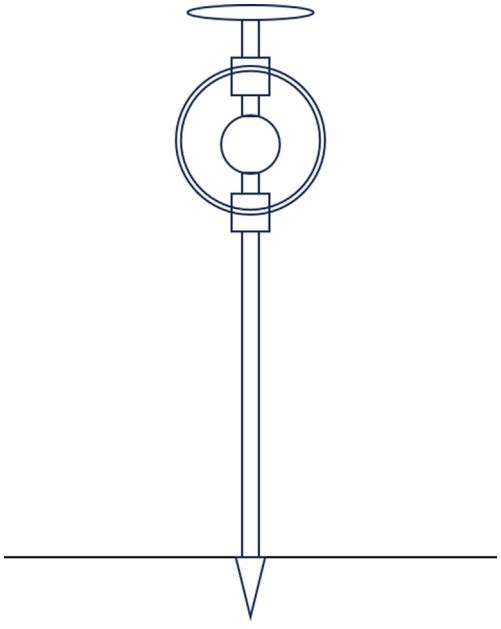

Fig. 18. Cone penetrometer apparatus. Redrawn from (Wong, 1989).

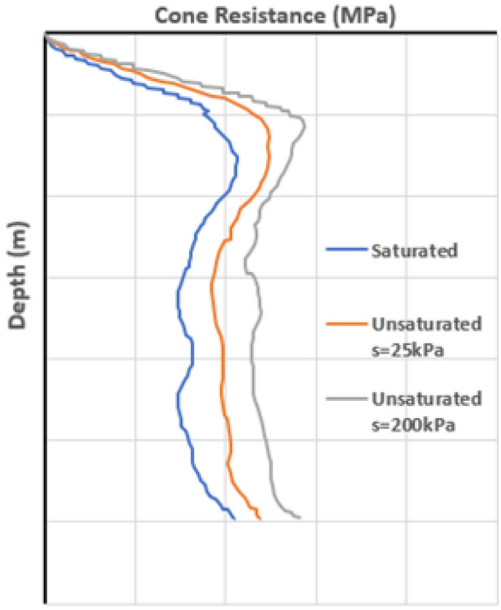

Fig. 19. Variation of cone resistance with soil saturation level. Redrawn from (Pournaghiazar et al., 2013).

priate constitutive material model must be selected. Over the years, many constitutive models based on elastic, elastic–plastic and elastic visco-plastic framework were developed for soil modeling and then implemented in commercial software. Some of these models are reviewed in the following sections.

3.1. Elastic constitutive models

The linear elastic model was the first choice due to its simplicity in simulating the soil behavior. While soil shear strain and volumetric strain are dependent on pore water pressure and effective stress, they are independent in the linear elastic model. Hence, nonlinear elastic models like bi-linear model (Potts et al., 2001), K-G model (Naylor et al., 1981) and hyperbolic model (Kondner, 1963) were introduced to overcome the shortcomings of linear elastic models.

Out of all non-linear soil models, hyperbolic model is used mostly due to its capability to define the stiffness based on the load path. Hyperbolic model can be implemented in FEM in incremental form using Hooke's law (Fig. 20). The original form of hyperbolic model was further developed for more broader application and it is known as 'Duncan-Chang' model (Duncan and Chang, 1970).

The original hyperbolic model equation was given as-

$$\sigma_1 - \sigma_3 = \frac{\varepsilon}{a + b\varepsilon} \tag{13}$$

where, σ_1 is major principal stress, σ_3 is minor principal stress, ε is axial strain and a and b are material constants. The model equation (Eq. (13)) represents a straight line and it is used to calibrate the model based on laboratory test data.

Hyperbolic models cannot handle critical soil behavior characteristics like dilation (i.e., volume expansion), strain softening behavior and irreversible deformation on loading at large strains (Potts et al., 2001; Brinkgreve, 2005). Soil-tool/tire interaction studies based on non-linear elastic models for soil are implemented with changing moisture content and strain rate effects, but they lack experimental validation (Alavi and Hojati, 2012). Because of the mentioned drawbacks, elastic-plastic models are more extensively used over elastic models in soil-tire/tool interaction studies.

3.2. Elastic-plastic constitutive models

Implementation of the principles of plasticity into elasticity made possible the simulation of soil permanent deformation, dilation and strain hardening or softening behavior. In an elastic–plastic material, total strain could be decomposed into elastic and plastic strain. The elastic region of the soil is usually very small (up to 0.1% strain) and can be computed from a linear elastic or hyperelastic constitutive model (Atkinson, 2000). The plastic response is usually calculated in terms of accumulated stress and incremental strain using yield function which determines the onset of the plastic behavior, flow rule which determines the direction of plastic increment and hardening law which governs the hardening/softening behavior of the material (Potts et al., 2001).

3.2.1. Yield function

A yield function (F) is defined for separating the pure elastic response from the elastic-plastic response. It is also a scalar function of the stress components or stress invariants, and the material plastic parameter k which controls the evolution of the yield surface. It governs the strain hardening or the softening response of the material and for elastic perfectly plastic material, its value is constant. If $F < 0$ then the response will be purely elastic (Fig. 21) and Elasto-plastic response for $F = 0$. While $F > 0$ is inadmissible, the yield surface can evolve with strain hardening and

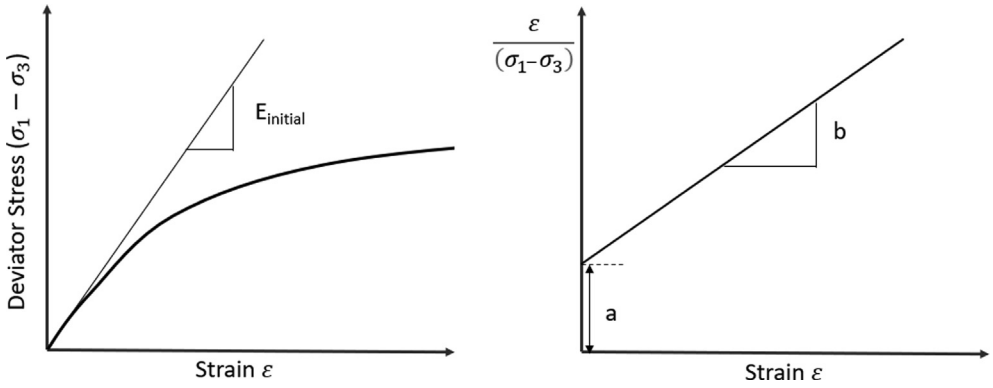

Fig. 20. Hyperbolic model stress–strain curve. Redrawn from (Duncan and Chang, 1970).

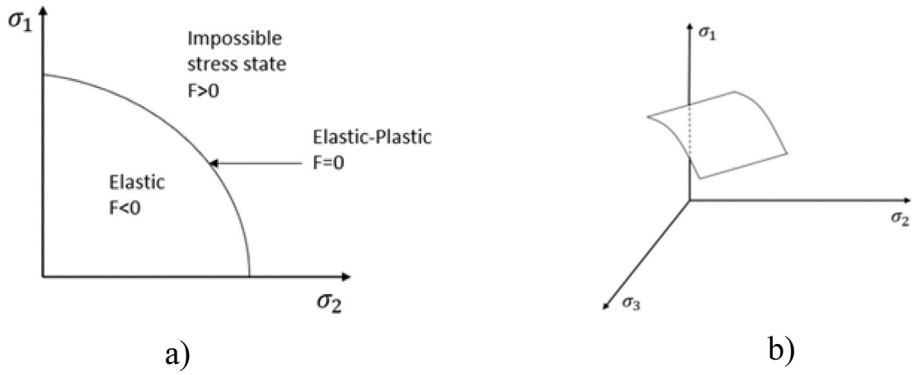

Fig. 21. a) Yield curve b) Yield surface segment. Redrawn from (Poodt et al., 2003).

previously inadmissible stress states can occur during deformation. For an isotropic material, the yield function can expressed in 3D space, but a 6D-hyperspace is required for an anisotropic material such as (Eq. (14))-

$$F = F(\sigma_{11}, \sigma_{22}, \sigma_{33}, \sigma_{12}, \sigma_{31}, \sigma_{32}, k) \tag{14}$$

The yield surface for the Mohr-Coulomb (MC) model is developed in 2D space using the failure criterion in terms of major and minor principal stresses (Eq. (15))(Fig. 22).The yield surface equations are also written in terms of stress invariants for capturing the general state of stress with more convenience (Eq. (16)) (De Borst et al., 2012). Discontinuous gradients of yield surface makes the solution unstable due to non-unique solution of plastic strain increments (Jiang and Xie, 2011). Researchers have modified the yield surface to make it smooth, however, it is computationally expensive (Hibbitt et al., 2013; Xiang and Zi-Hang, 2017). Yield surface of MC model can be easily calibrated using results of simple laboratory (direct shear test) or in-situ test (cone penetrometer test).

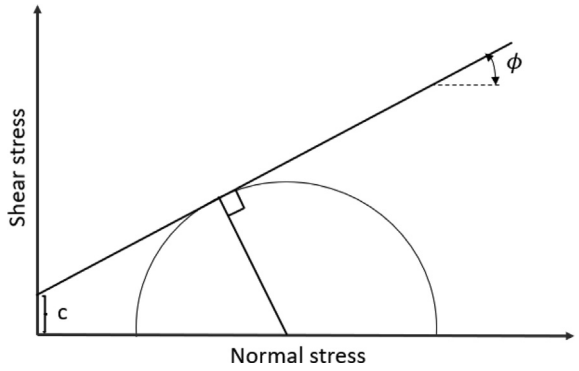

Fig. 22. Yield surface of Mohr Coulomb model. Redrawn from (Hibbitt et al., 2013).

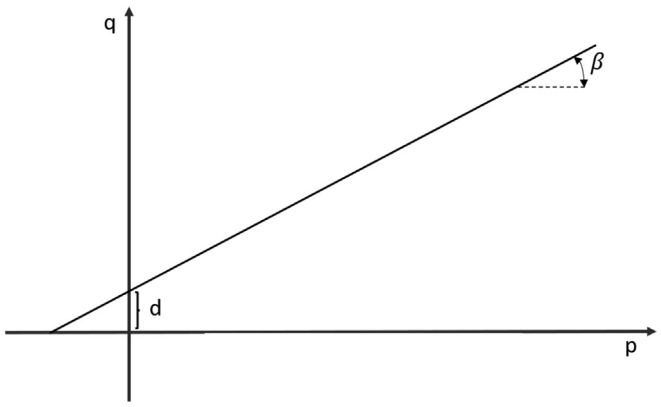

Fig. 23. Yield surface of Drucker Prager model in p-q space. Redrawn from (Hibbitt et al., 2013).

$$F(\sigma, k) = \frac{1}{2}(\sigma_1 - \sigma_3) - ccos\phi - \frac{1}{2}(\sigma_1 - \sigma_3)\sin\phi \tag{15}$$

$$F(\sigma, k) = \left(\cos\theta - \frac{1}{\sqrt{3}}\sin\theta\sin\phi\right)\sqrt{J_2} + I_1\sin\phi - c\cos\phi \tag{16}$$

Drucker-Prager (DP) with smooth cylindrical cone yield surface was proposed to address the instabilities in Mohr-Coulomb yield surface (Drucker et al., 1952). The yield surface is expressed in terms of stress invariant in p-q space (Eq. (17)) (Fig. 23). DP and MC yield surfaces can be compared by aligning the apex of both yield surfaces and relations between material parameters of both models can be established (Eq. (18) & Eq. (19)). DP model unlike MC model consider the contribution of intermediate stress in the material failure (Chen, 2007). One of the major limitation of linear DP model is it fails to capture the behavior of material when it is loaded or unloaded along hydrostatic axis (Drucker et al., 1957). DP yield surface can be readily calibrated using MC model parameters or through simple laboratory (direct shear test) or in-situ test (cone penetrometer test).

$$F(\sigma) = q - 3\sqrt{3}\alpha p - \sqrt{3k_2} \tag{17}$$

$$\alpha = \frac{3sin\phi}{\sqrt{3}(3 - sin\phi)} \tag{18}$$

$$k_2 = \frac{6\cos\phi}{\sqrt{3}(3 - \sin\phi)} \tag{19}$$

In order to improve the behavior of DP model, an elliptical cap was introduced to the original cone yield surface (DiMaggio and Sandler, 1971). The modified or extended Drucker-Prager (MDP) model yield surface is divided into three segments: a shear surface (Eq. (20)), an elliptical cap that intersects hydrostatic line at right angle (Eq. (21)) and a transition surface between shear failure sur-

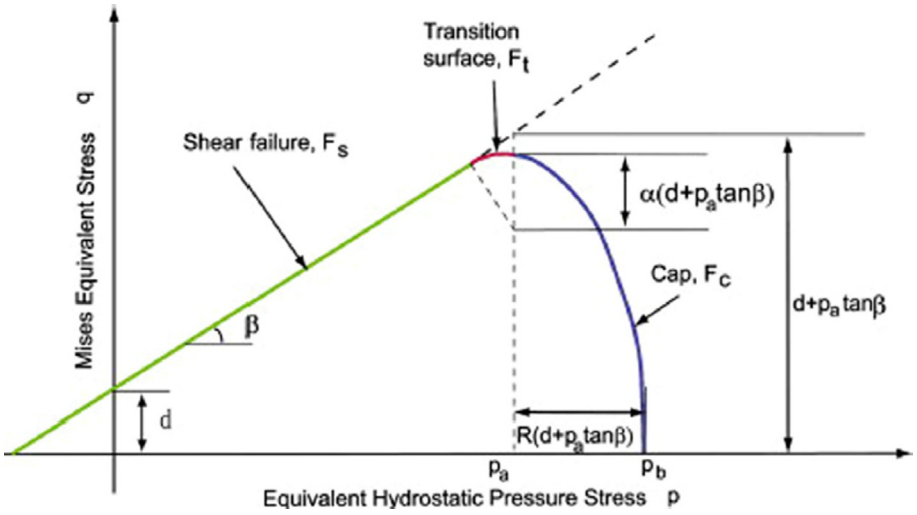

Fig. 24. Modified Drucker Prager yield surface in p-q space (Trower et al., 2023).

face and cap to avoid any discontinuity in the overall yield surface (Eq. (22)) (Fig. 24). MDP yield surface requires laboratory test data (triaxial test) for calibration.

$$F_s = t - ptan\beta - d = 0 \tag{20}$$

$$F_c = \sqrt{(p - P_a)^2 + \left[\frac{Rt}{1 + \alpha - \alpha/\cos\beta}\right]^2} R(d + P_a tan\beta) = 0 \tag{21}$$

$$F_t = \sqrt{(p - P_a)^2 + \left[t - \left(1 - \frac{\alpha}{\cos\beta}\right)(d + P_a tan\beta)\right]^2} - \alpha(d + P_a tan\beta) = 0 \tag{22}$$

Unlike yield surfaces based on metal plasticity concepts discussed earlier, Cam-Clay (CC) and modified Cam-Clay model (MCC) yield surfaces were developed based on critical soil mechanics concepts using triaxial test results of saturated clays (Roscoe et al., 1963; Roscoe and Burland, 1968; Schofield and Wroth, 1968) (Fig. 25). The yield function of CC model plots as logarithmic curve (Eq. (23)), but it has inherent discontinuity at zero deviatoric stress which is difficult to handle in numerical implementation. Hence, MCC is developed with elliptical curve in p-q space to overcome the limitations of original CC model (Eq. (24)). These models usually overpredict the failure stress for highly over-consolidated soils and usually corrections have to be made to the yield surface, which cannot be readily done in commercial FE codes. Calibration methodology to CC and MCC yield surfaces is similar to MDP yield surface.

$$F(\sigma, k) = \frac{q}{Mp'} + ln\left(\frac{p'}{p'_c}\right) = 0 \qquad \text{(CC)} \tag{23}$$

$$F(\sigma, k) = \left(\frac{q}{Mp'}\right)^2 - \left(\frac{p'_c}{p'} - 1\right) = 0 \quad \text{(MCC)} \tag{24}$$

These are some of the yield surfaces that can be readily implemented in commercial FE software. The proper yield surface must be chosen based on the test data available and the type of soil, as these factors have a considerable impact on the stability and correctness of the numerical solution.

3.2.2. Flow rule

The flow rule indicates how the yield surface will evolve during plastic straining at each stress state using plastic potential function (G) and plastic multiplier (λ_1) (Eq. (25)). Plastic potential function is a surface in stress space that is perpendicular to the plastic strain increment. In classical plasticity theories, it was assumed that the yield function is same as plastic potential function i.e., associative flow rule ($F = G$) (Fig. 26-a). But through test data, it was concluded that for the frictional materials (e.g., soil), the plastic potential function is different than yield surface i.e., non-associative flow rule ($F \neq G$) (Fig. 26-b) (Kim and Lade, 1988). Non-associative flow rule might cause the loss of strong ellipticity to the yield surface and violate Drucker stability postulate for certain stress paths during strain softening phase, hence this should be checked during implementation of non-associative flow rules as this will affect the numerical stability of the simulation (De Borst, 1986; Bigoni and Zaccaria, 1992).

$$\Delta\varepsilon_{ij}^{p} = \lambda_1 \frac{\partial G}{\partial \sigma_{ij}} \tag{25}$$

MC and DP models can be implemented with associative or non-associative flow rules depending on the material behavior in the majority of commercial FE programs. In p-q space, the plastic

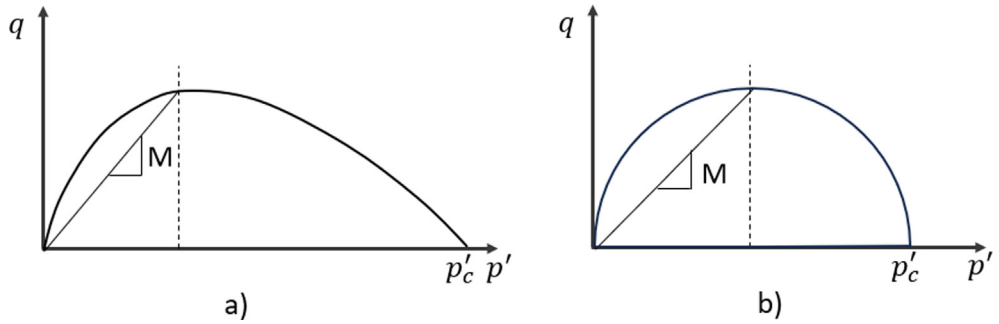

Fig. 25. Yield curves-a) Cam-Clay and b) Modified Cam-Clay. Redrawn from (Puzrin, 2012).

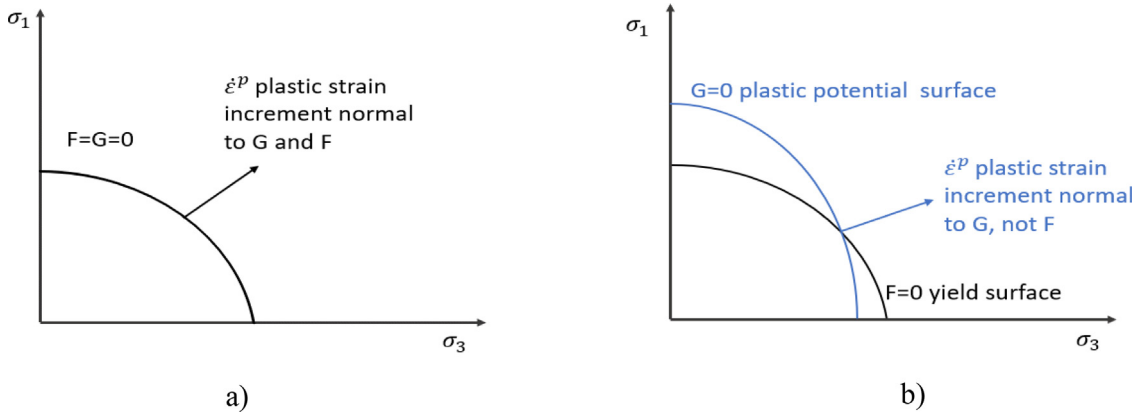

Fig. 26. a) Associative flow rule b) non-associative flow rule. Redrawn from (Poodt et al., 2003).

potential function for the MC model is a hyperbolic function, while for the DP model it is a linear function. The plastic potential functions of both models are calculated using yield surface parameters and dilation angle. Dilation angle of material is typically calculated by laboratory testing or calibrated using optimization tools (Sumelka, 2014; Systemes, 2015; Xiang and Zi-Hang, 2017).

In MDP model, associative flow rule is used for the cap yield surface, therefore the plastic potential function is same as yield function. At the shear surface, non-associative flow rule is used with elliptical plastic potential function (Eq. (26))(Fig. 27) (Hibbitt et al., 2013). Unlike, MC model and DP model, the dilation angle is not fixed but it is estimated based on the state of hydrostatic stress and volumetric strain. This non-associative flow rule formulation can capture the behavior of dilative material for which dilation angle varies significantly based on relative density and stress state (Lings and Dietz, 2005).

$$G_s = \sqrt{[(P_a - p)tan\beta]^2 + \left[\frac{q}{1 + \alpha - \alpha/cos\beta}\right]^2} \tag{26}$$

CC and MCC model formulation are implemented with associative flow rule. With associative flow rule, these models cannot predict the peak stresses observed in the undrained test of some loose sands and undisturbed normally consolidated clays. Further, it makes calibration for granular materials difficult compared to clays (Yu, 1998).

Based on the formulation of the constitutive models, either associative, non-associative or combination of both flow rules are available. The use of non-associative flow rule is quite costly as it results in non-symmetric constitutive matrix, hence based on the soil type appropriate formulation should be used.

3.2.3. Hardening/Softening law

Flow rule gives details regarding the direction of plastic strain increment i.e., the direction in which yield surface should evolve but the magnitude of the plastic strain increment is governed by the plastic multiplier (λ_1). Plastic multiplier is quantified using the hardening parameter k defined with yield surface. Hardening law describes how hardening parameter k changes with plastic strain (Fig. 28-a&c). For perfectly plastic materials, k is constant and there is no hardening or softening rule defined (Fig. 28-b). Different constitutive models associate hardening parameters with plastic or volumetric strains and plastic work. In the theory of plasticity, isotropic hardening, kinematic hardening, and combined hardening are defined. Isotropic hardening is usually considered in most of the constitutive models because of its mathematical simplicity compared to kinematic hardening though doesn't reflect the realistic behavior of the soil (Scott, 1985).

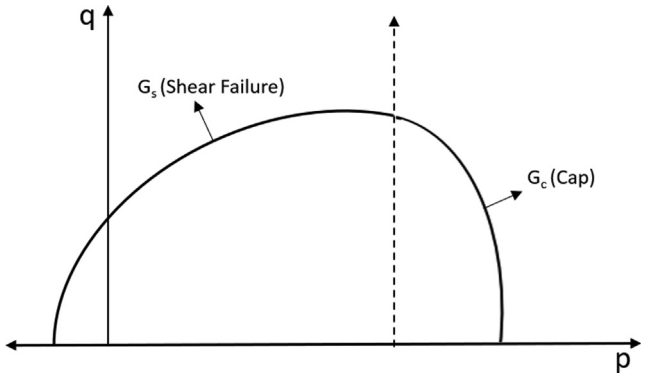

Fig. 27. Plastic potential function of modified Drucker Prager model. Redrawn from (Shoop et al., 2005).

As there is no hardening/softening law incorporated in the MC model, its behavior is elastic-perfectly plastic. A hardening law based on test results can be applied to the DP model or it can be utilized as an elastic-perfectly plastic model. Like this, the user determined hardening rule based on compressive hydrostatic yield stress and plastic volumetric strain is employed with the MDP model. For CC and MCC models the hardening and softening is a function of the plastic volumetric strain, swelling index and compression index. All of the discussed constitutive models need the results from laboratory consolidation tests (Oedometer tests) in order to be completely calibrate with the hardening/softening law (Hibbitt et al., 2013).

To summarize, elastic-plastic constitutive models need yield surface and flow rule definition with optional hardening/softening law. A suitable constitutive model should be selected based on the required output of the soil-tire/tool interaction studies and type of soil to be modeled. Simple models like DP and MC can predict the soil deformation and interface forces with reasonable accuracy compared to experimental data in earth moving and traction studies. DP and MC models being elastic perfectly plastic models cannot predict accurate soil stresses under hydrostatic and dynamic conditions which is the focus of soil compaction studies (Li and Schindler, 2013; Ucgul et al., 2018; Zhang et al., 2018; Farhadi et al., 2019). Validated advanced elastic-plastic model such as MDP is capable of predicting soil stresses, soil deformation and interface forces (Chiroux et al., 2005; Cueto et al., 2013). CC and MCC models have limited applicability in these studies though they consider the effect of soil stress history because it is not able to capture the behavior of dilative and loose soils (Adams, 2002). Elastic-plastic constitutive models developed in recent years such as Hardening soil model which is similar to MDP but with additional hardening law for shearing and NorSand model which addresses the shortcomings of MCC can also be considered in future soil-tire/tool interaction studies (Jefferies and Shuttle, 2005; Benz et al., 2008).

3.3. Elastic-plastic constitutive models for unsaturated soils

As per previous discussion (Section 2), mechanical properties of soil like compressibility and shear strength are dependent on the matric suction (moisture content). The parameters of elastic-

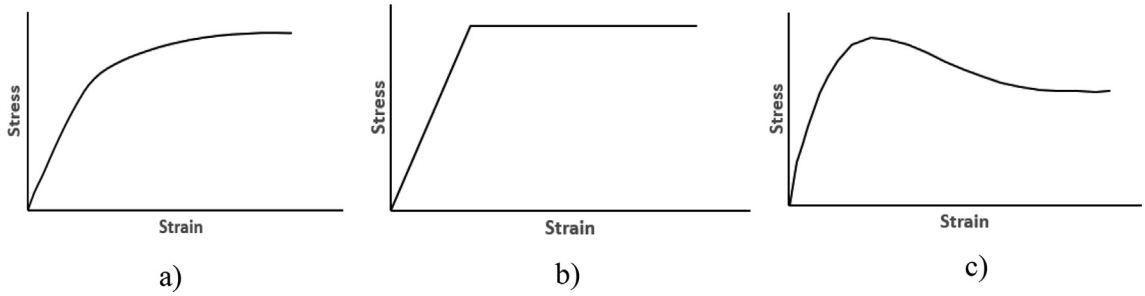

Fig. 28. a) Strain hardening, b) elastic perfectly plastic and c) strain softening. Redrawn from (Smed and Cundall, 2012).

plastic models for unsaturated soils are estimated based on total stress approach (TSA) or effective stress approach (ESA). TSA is suitable and simple to implement compared to later for short-termload application problems like majority of soil-tire/tool interaction studies. However, there is still no clear recommendation or comparison provided in the literature between both of these approaches for medium to long-term loading problems such as tire or tool multiple runs over the same soil (Day, 2001). Material model parameters based on TSA are estimated based on UU triaxial test of soil at different moisture content. While for estimating ESA parameters, long-term CD or CU triaxial test data with pore water and pore air measurements is required (Wulfsohn et al., 1998).

In soil-tire/tool interaction studies, TSA based elastic–plastic models such as MC and DP models have been implemented and validated against soil deformation and interface forces experimental data (Cueto et al., 2013; Tagar et al., 2015; Farhadi et al., 2019). Validation of these material models against soil stress measurements at different depths with different moisture content is yet to be undertaken. Further, the use of TSA compared to ESA for non-cohesive soil, itself is debated. The assumption of undrained behavior for short term loading for non-cohesive soils may induce some error in the soil compaction prediction and this may be verified with the modeling of such soils using both approaches and correlating the results with experimental data (Schanz et al., 2010).

For simulation of dry, fully saturated soils using ESA and TSA as well as unsaturated soils with TSA can be done using commercial software such as ABAQUS, LS-Dyna, and ANSYS. These commercial FEA codes are unable to simulate unsaturated soils using ESA; instead, user-defined material models has to be used (Prajapati and Das, 2023). Many geotechnical applications focus on unsaturated soils, therefore commercial geotechnical codes like PLAXIS and COMSOL readily provide ESA-based elastic-plastic models like the Barcelona Basic model (Brinkgreve et al., 2016). These software can be useful for studies related to unsaturated soils even though their applicability in soil-tire/tool interaction is limited (Alavi and Hojati, 2012).

3.4. Elastic-visco-plastic constitutive models

For dynamic conditions like soil-tire/tool interaction, some types of soils exhibit strain rate-dependent behavior which can be better predicted with elastic-viscoplastic constitutive models rather than constitutive models based on elasticity, hypoplasticity, plasticity and endochronic theories (Prevost and Popescu, 1996). Through experimental studies, it is evident that saturated cohesive soils have rate-dependent behavior but for unsaturated cohesive soils and cohesionless soils, rate-dependency cannot be concluded readily. For such soils, rate-dependent behavior is dependent on the mineral composition, moisture content and permeability (Karafiath and Sobierajsku, 1974).

Basic viscoplasticity formulation on which most of the elasto-viscoplastic models are formulated assumes the total strain rate is the summation of elastic strain rate, which is independent of the strain rate, and viscoplastic strain rate which is a function of the excess stresses above the static yield criterion (Eq.(27) & Eq. (28)).

$$\dot{\varepsilon}_{ij} = \dot{\varepsilon}^{e}_{ij} + \dot{\varepsilon}^{vp}_{ij} \tag{27}$$

$$\dot{\varepsilon}^{vp}_{ij} = \eta\langle\phi(F)\rangle\frac{\partial G}{\partial\sigma_{ij}} \tag{28}$$

where, $\dot{\varepsilon}^{vp}_{ij}$ is viscoplastic strain rate, η is viscosity constant of the material, $\langle\phi(F)\rangle$ is viscous flow function, $\frac{\partial G}{\partial\sigma_{ij}}$ is flow direction of the viscoplastic strain rate and G is the plastic potential function and σ_{ij} is the stress tensor. The viscous flow function can be determined based on the dynamic testing of the material or assumed to be predetermined overstress function of the general yield criterion. Linear, exponential and power functions are some of the extensively used overstress functions (Perzyna, 1966).

The static yield function (F), can be used with any elastic–plastic yield function. For isotropic hardening, the yield function is given as (Eq. (29))-

$$F(\sigma_{ij}, \varepsilon^{vp}_{kl}, k) = \frac{f(\sigma_{ij}, \varepsilon^{vp}_{kL})}{k\left(\varepsilon^{vp}_{k_l}\right)} - 1 \tag{29}$$

where $f(\sigma_{ij}, \varepsilon^{vp}_{kL})$ is function of stress tensor and viscoplastic strains. $k\left(\varepsilon^{vp}_{k_l}\right)$ is the hardening parameter dependent on the viscoplastic strain.

Elastic-viscoplastic constitutive models are available in the material library of the common commercial software used in soil-tire/terrain studies like ABAQUS and LS-Dyna. For calibration of these material models, triaxial or direct shear test data at different strain rates is required. Because of the difficulty in obtaining strain rate-dependent testing data and complexity of calibrating large number of parameters, large scale use of these models in terramechanics applications is not witnessed (Saliba, 1990; Armin et al., 2017). The variation in the output of studies utilizing elastic viscoplastic formulations compared to elastic-plastic formulations is not quantified yet and it is still an area of open research.

4. Soil-Tire/Tool interaction studies

For the study of soil-tire/tool interaction, various approaches like empirical, semi-empirical, analytical, continuum mechanics-based methods (with and without mesh), discrete element methods were used in the past. These methods are briefly discussed in the next sections.

4.1. Empirical methods

Modeling of soil interaction simulations is quite complex and requires extensive testing for the characterization of the soil properties. To simplify that, empirical methods with simple field measurement data were used to study tool and tire performance on different soils. Using these empirical relations, draft forces for tillage tools, soil compaction and trafficability were estimated for different types of soil.One of the earliest, empirical method was based on vehicle cone index (VCI), which is measured using cone penetrometer. For example, WES (Waterways Experiment Station) VCI model was developed for predicting vehicle performance on fine and coarse-grained organic soils (Rula and Nuttall Jr, 1971). Trafficability of the vehicle, without getting incapacitated based on number of passes made, is calculated using VCI which is directly dependent on the mobility index.

Empirical methods results are highly dependent on the vehicle and soil type for which test data is available. If there are significant changes to the tested conditions, the results cannot be extrapolated for that, which is one of the major drawbacks of empirical relations. Though empirical methods provide good preliminary estimations of vehicle performance, they cannot be used for broader scopes such as vehicle development and design. For detailed studies, more sophisticated methods such as semi-empirical or numerical approaches should be used (Wong, 2022).

4.2. Semi-empirical and analytical methods

To overcome the limitations of empirical methods and reduce the testing effort required for soil characterization, semi-empirical and analytical methods were developed. Most of these

methods are based on the classical soil mechanics and theory of plasticity principles.

4.2.1. Soil-tire interaction models

For given input of vehicle and soil parameters, vehicle mobility parameters such as drawbar pull, motion resistance etc. can be calculated using these semi-empirical and analytical methods. In terramechanics, pressure-shrinkage and shear stress-displacement relationships characterize the soil properties. Using these relationships, resistive forces and traction forces can be predicted and the results can be validated through draw bar pull test (Eq.(30)) (He et al., 2019).

$$F_D = F_T - \sum R \tag{30}$$

where, F_D is drawbar pull force, F_T is the thrust force and $\sum R$ is summation of all resistive forces (i.e., soil compaction, bulldozing, tire deformations, etc.).

Pressure sinkage relationship provides the estimate of the resistive forces between tire and soil due to soil compaction. Bekker and Reece pressure sinkage relationships are used extensively in analysis of vehicle performance over different types of soils (Bekker, 1956; Reece, 1965). Bekker model (Eq. (31)) considers the effect of cohesion and internal resistance of soil on pressure sinkage relationship, while Reece model (Eq. (32)) is based on Terzaghi's bearing capacity equation. For calibration of both models, bevameter is used which can measure the soil response to normal and shear loads. Later, several modifications are made to these fundamental equations to consider the effect of tire shape, slip at soil-tire interface and steering moment (Gee-Clough, 1976; Wong et al., 1984; Ding et al., 2014).

$$P = \left(\frac{k_c}{b} + k_\phi\right) z^n \tag{31}$$

$$P = \left(ck'_c + \gamma_S b k'_\phi\right)(z/b)^n \tag{32}$$

where P is pressure, z is sinkage, b is geometry dimension, n, k_c, k_ϕ are pressure sinkage parameters for Bekker model, k'_c, k'_ϕ are pressure sinkage parameters for Reece model, γ_S is the weight density of soil and c is the cohesion of the soil. Based on Bekker pressure sinkage relation, rolling resistance force for the towed, rigid tire was calculated as follows (Eq. (33))-

$$R_c = \frac{1}{(n+1)\left(k_c + bk_\phi\right)^{1/n}} \left(\frac{W}{L}\right)^{\frac{n+1}{n}} \tag{33}$$

where R_c is rolling resistance force due to soil compaction, W is vertical load and L is length of loaded area.

The shear stress-shear displacement relationship estimates the tangential force acting at the tire-soil interface which is also known as thrust force. MC failure criterion and its modified versions for unsaturated soils are extensively used in the development of analytical and semi-empirical models. Two classes of shear stress-shear displacement models are developed, one for the soils showing peak shear stress values (i.e., dilative soils) and other for soils without distinctive peak behavior. Bekker model (Eq. (34)) for soils with peak shear stress and Janosi model (Eq. (35)) for soils without peak shear stress are one of the fundamental models used extensively (Bekker, 1956; Janosi and Hanamoto, 1961).

$$\tau = \tau_{max} \frac{\left\{\exp\left[\left(-K_2 + \sqrt{K_2^2 - 1}\right)K_1 j\right] - \exp\left[\left(-K_2 - \sqrt{K_2^2 - 1}\right)K_1 j\right]\right\}}{\left\{\exp\left[\left(-K_2 + \sqrt{K_2^2 - 1}\right)K_1 j_0\right] - \exp\left[\left(-K_2 - \sqrt{K_2^2 - 1}\right)K_1 j_0\right]\right\}} \tag{34}$$

$$\tau = \tau_{max}[1 - \exp(-j/K)] \tag{35}$$

where τ is the shear stress, j is the shear displacement, τ_{max} is the shear strength estimated using MC failure criterion, j_0 is the shear displacement at the maximum shear stress, K_1 and K_2 are empirical constants and K is the shear deformation modulus.

Numerical models are used extensively because of their ability of capturing all modes of soil deformation and stress distribution at the tire-soil interface accurately compared to semi-empirical and analytical models (Ma et al., 2009). However, limited numerical models-based studies for multipass effects and mobility over unsaturated soils are available because of the modeling complexity of multiphase soil behavior with accurate hardening laws. The semi-empirical and analytical models can be used in predicting performance for such cases and also can be coupled in real time system because of its simplicity (He, 2020).

4.2.2. Soil-tool interaction models

Semi-empirical and analytical models to predict the draft forces during tillage operations were developed based on Terzaghi's passive earth pressure theory. Based on the classical soil mechanics principles, these models proposed different soil failure patterns and based on that soil forces equations were derived.

For estimating the soil forces on wide tools, two-dimensional analytical soil tool interaction models are used. First, based on the dimensional analysis, the factors affecting the soil tool interaction were identified. Later, based on the identified variables, general earth pressure equation was proposed. One of the limitations of two-dimensional models was they were not able to predict the forces from narrow tillage tools accurately, hence these models were extended to three dimensional models (Kushwaha et al., 1993). Payne's model (Payne, 1956) is based on the top soil surface failure zone, Hettiaratchi-Reece model (Hettiaratchi and Reece, 1967) is based on different soil failure configurations, Swick-Perumpral model (Swick and Perumpral, 1988) with consideration of tool traveling speed and Zeng-Yao model (Dechao and Yusu, 1992) with consideration of damping effect on the shear strain rate and shear strength relation are some well-known of the three-dimensional soil tool interaction models used in different soil-tool interaction studies.

4.3. Finite-element methods

FE methods are used extensively for numerical modeling of soil, because of their advantage of capturing the deformations and stresses in a more detailed manner and ease of handling complex boundary conditions and contact interfaces. Further, these methods allow to capture the behavior of soil with good accuracy with the help of advanced material constitutive relations which can be calibrated with relatively simple soil tests.

In Lagrangian formulation, each node of the mesh follows the assigned material particle during the deformation (Fig. 29). It is easy to track the material boundary, free surfaces, and different interfaces with well-defined contact algorithms. It also allows to track the history dependent internal variables required for solving material constitutive equations. However, the large mesh distortions of the Lagrangian formulation add sensitivity and instability to the FE solution without frequent remeshing operations. This remeshing procedure is quite computationally expensive to implement and degrades the solution also because of the mapping of solution variables to new mesh at every time step (Boman and Ponthot, 2004).

Eulerian mesh formulations are used extensively in the field of aerospace and fluid mechanics. Contrary to Lagrangian formulations, the mesh is not associated with the material particles, the continuum can freely flow through the mesh (Fig. 29). This formu-

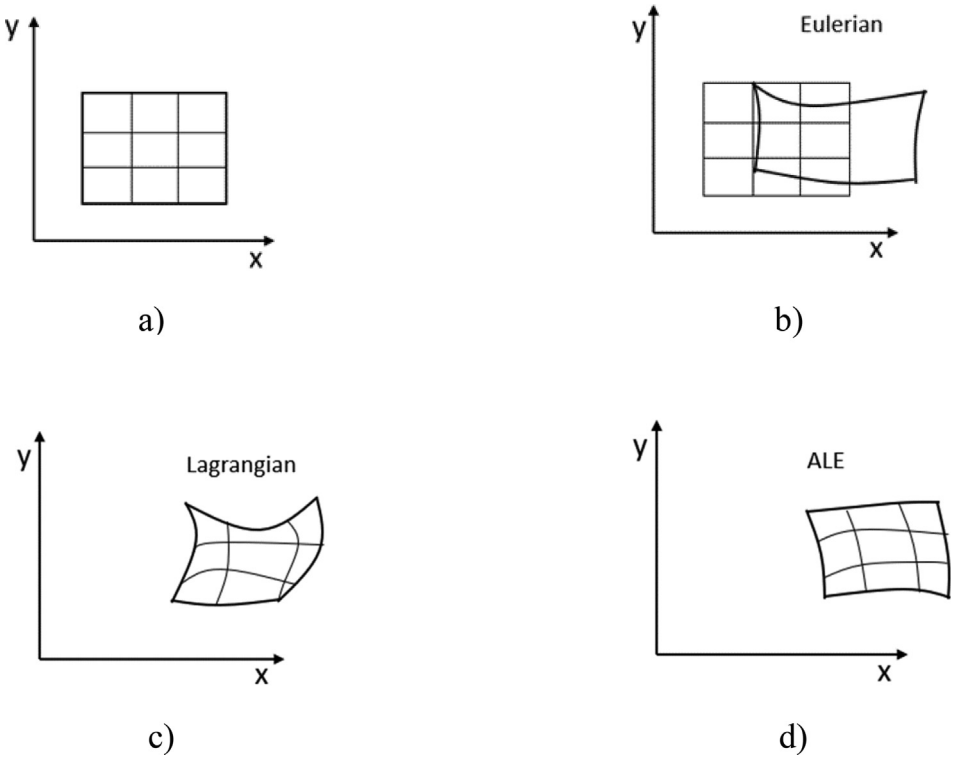

Fig. 29. a) Undeformedbody, b) Deformation based on Eulerian formulation, c) Deformation based on Lagrangian formulation and d) Deformation based on ALE formulation. Redrawn from (Boman and Ponthot, 2004).

lation overcomes the limitations of excessive mesh distortion, but it has difficulties in tracking the different material interfaces. Further, it is quite difficult to model cohesive soils with friction and plasticity using Eulerian methods compared to Lagrangian formulation.

ALE (Arbitrary Lagrangian-Eulerian) mesh formulations are developed to overcome the limitations of pure Lagrangian and Eulerian formulations. The mesh may move with continuum like Lagrangian formulation, it can be fixed like Eulerian formulation, or it can move separately (Fig. 29). This method accommodates more distortions than Lagrangian method and provides better resolution of material interfaces than Eulerian method. ALE formulations can be implemented as direct solution of continuum balance equations or operator split algorithm. Commercial FE codes uses the latter, where ALE formulation is implemented in two stages (Fig. 30). First is Lagrangian stage where mesh moves with the material and second stage is advection phase where deformed mesh is remapped to initial position for ALE formulation.

4.3.1. Soil-tire interaction studies

For soil-tire interaction studies, FEM is used extensively as it is compatible with variety of elastic, elastic–plastic and elastic-viscoplastic material models which are directly calibrated using soil testing data. FEM is widely used and validated for predicting the soil compaction, drawbar pull and soil stresses under tire at different normal loads, inflation pressure, slip ratios and soil moisture content (Table 2) (Fervers, 2004; Farhadi et al., 2019; Swamy et al., 2023).

Though FEM is the preferred option for majority of computational mechanics problems, it has several disadvantages in context of simulating soil-tire interaction. Because it is a meshed method, influence of local failure and soil flow under the tire cannot be modeled accurately. This results in difficulty of predicting the wheel sinkage at higher slip ratios especially for cohesionless soils (Hambleton, 2010). In literature, implementation of validated elastic-viscoplastic models with focus on soil-tire interaction studies is not available. In general, FEM is suitable for majority of soil-

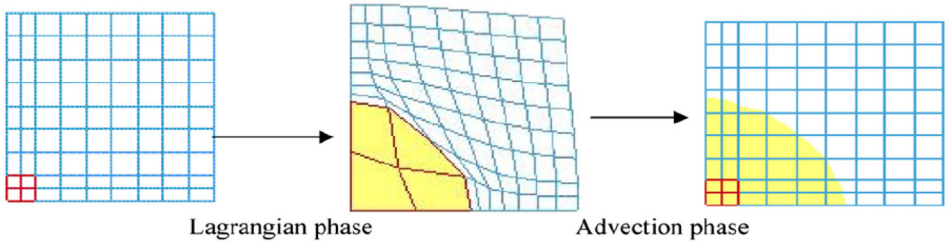

Fig. 30. Operator Split algorithm for ALE formulation implementation (Souli and Shahrour, 2012).

Table 2
Overview of FEM based soil-tire interaction studies.

Author	Software	Soil Material Model	Meshing Formulation	Research Focus
(Fervers, 2004)	ABAQUS	Cap plasticity	Lagrangian	Soil compaction on different soils
(Chiroux et al., 2005)	ABAQUS	Cap plasticity	Lagrangian	Stresses at tire-soil interface
(Du et al., 2017)	ABAQUS	Drucker–Prager	Lagrangian	Stresses at tire-soil interface
(Papamichael, 2019)	ABAQUS	Drucker-Prager	Lagrangian	Energy dissipation during braking and driving on soft soil
(Xia, 2011)	ABAQUS	Cap plasticity	Lagrangian	Contact force and stresses at tire soil interface
(Deng et al., 2019)	ABAQUS	Cap plasticity	Lagrangian	Soil compaction and tire deformation
(Ma et al., 2009)	ABAQUS	Cap plasticity	Lagrangian	Contact force and stresses at tire soil interface
(Liu and Wong, 1996)	MSC MARC	Cam Clay	Lagrangian	Drawbar performance of tire on Ottawa sand
(Li and Schindler, 2013)	ABAQUS	Cap plasticity	Lagrangian	Effect of axle load and tire inflation pressure on rolling resistance and soil compaction
(Cueto et al., 2013)	ABAQUS	Cap plasticity	Lagrangian	Soil compaction caused by agricultural tire
(Farhadi et al., 2019)	ABAQUS	Drucker-Prager	Lagrangian	Effect of soil moisture on soil compaction and tire sinkage
(Abu-Hamdeh and Reeder, 2003)	User defined solver	Duncan Chang	Lagrangian	Stress distribution at traction device-soil interface
(Oida et al., 2005)	MSC DYTRAN	Mohr Coulomb	Eulerian	Drawbar performance of the tire with different slip ratios
(Wright, 2012)	LS DYNA	Pseudo-tensor Soil and Foam	Eulerian	Drawbar pull simulations of tire at different normal load and inflation pressure
(Hambleton and Drescher, 2009)	ABAQUS	Von-mises plasticity	ALE	Contact area and stress of rigid wheel and cylinder rolling on deformable terrain
(Bekakos et al., 2015)	ABAQUS	Drucker-Prager	ALE	Tire sinkage at different loads and slip ratios
(Shoop et al., 2005)	ABAQUS	Cap plasticity	ALE	Drawbar pull simulation tire rolling on thawed soil
(Bekakos et al., 2017)	ABAQUS	Drucker-Prager Mohr coulomb	ALE	Tire sinkage at different loads and slip ratios with different material models
(Obermayr et al., 2010)	ABAQUS	Cap plasticity	Eulerian	Tire sinkage and drawbar pull performance simulations
(Yamashita et al., 2018)	User defined solver	Drucker-Prager	Lagrangian (Locked element formulation)	Tire sinkage simulations at different normal loads

tire interaction simulations for cohesive soils, however, use of particle-based methods is recommended for studies interested in simulating cohesionless and strain rate dependent behavior of soils (Hu et al., 2021).

4.3.2. Soil tool interaction studies

In Soil-tool interaction studies, finite element methods are extensively used because of increased computation power and limitations of analytical models in predicting the interaction of narrow and complicated tool geometries with soil (Chi and Kushwaha, 1990). FEM was implemented with different elastic, elastic-plastic and elastic viscoplastic materials models to predict draft and vertical forces of different tools with changing tool speed, tool size and rake angle (Table 3). Majority of these studies are validated with experimental data in terms of cutting forces or soil flow patterns (Abo-Elnor et al., 2004; Armin et al., 2017). However, FEM has difficulty in modeling the crack formation, crack propagation and soil fragmentation that usually occurs during soil cutting process, resulting in overprediction of draft forces. Particle-based methods are better at predicting draft forces with reasonable accuracy but compared to them, FEM is still relatively simple and can be easily calibrated with limited test data (In-situ test) to study soil-tool interaction particularly in case of cohesive and unsaturated soils (Mouazen and Neményi, 1999; Alavi and Hojati, 2012).

4.4. Particle-based methods

Particle-based methods employ both continuum (e.g., smoothed particle hydrodynamics (SPH), Material point method) and discrete (e.g., discrete element methods) approaches to describe the behavior of granular materials. Contrary to FEM approach, the approximations of the field variables are dependent on the particles and not on the element based on discretized mesh. In continuum approach of particle-based methods, the domain of influence of each particle is defined for calculating inter particle interactions. This domain of influence and neighboring particles

Table 3
Overview of FEM based soil-tool interaction studies.

Author	Software	Soil Material Model	Meshing Formulation	Research Focus
(Chi and Kushwaha, 1990)	SOIL 3D	Duncan-Chang	Lagrangian	Soil cutting forces, stresses, and displacement
(Kushwaha and Shen, 1995)	User defined solver	Qun-Shen	Lagrangian	Soil tool interaction at different speeds
(Fielke, 1999)	NISA	Mohr-Coulomb	Lagrangian	Effect of tool geometry on tillage forces
(Mouazen and Neményi, 1999)	COSMOS	Drucker Prager	Lagrangian	Tool forces and stresses in non-homogenous soil
(Abo-Elnor et al., 2004)	ABAQUS	Hypoplastic	Lagrangian	Effect of mesh density, tool width and soil swelling on soil cutting forces
(Alavi and Hojati, 2012)	PLAXIS	Duncan-Chang	Lagrangian	Effect of tool forward speed, rotary speed, and soil moisture content on soil stresses
(Tagar et al., 2015)	LS-DYNA	FHWA soil	Lagrangian	Comparison of soil failure pattern with experimental results
(Li et al., 2015)	ABAQUS	Drucker Prager	Lagrangian	Effects of rotary speed on soil cutting speed
(Armin et al., 2017)	ANSYS	Drucker-Prager	Lagrangian	Draft forces and soil flow pattern
(Ucgul et al., 2018)	NISA	Mohr Coulomb	Lagrangian	Soil tool interaction forces
(Karmakar et al., 2009)	CFX	Bingham	Eulerian	Effect of tool speed and soil moisture content on draft forces
(Zhu et al., 2017)	ANSYS	Bingham	Eulerian	Effect of tool speed and operational depth on draft forces
(Zhang et al., 2018)	ABAQUS	Drucker-Prager	ALE	Effect of cutting angle and depth on draft force

Table 4
Overview of SPH based soil-tire interaction studies.

Author	Software	Soil Material Model	Research Focus
(El-Gindy et al., 2011)	PAMCRASH	Elastic-plastic hydrodynamic	Pressure sinkage and shear displacement correlation between SPH and FEA models
(Ragheb et al., 2013)	PAMCRASH	Elastic-plastic hydrodynamic	Tire's rolling resistance, vertical stiffness, and steering characteristics on soft soil
(Dhillon et al., 2013)	PAMCRASH	Elastic-plastic hydrodynamic	Effect of tire inflation pressure and vertical load on rolling resistance on different soils
(El-Sayegh et al., 2018)	PAMCRASH	Elastic-plastic hydrodynamic	Effect of soil moisture content on rolling resistance performance of tire on different soils
(Gheshlaghi et al., 2021)	PAMCRASH	Elastic-plastic hydrodynamic	Tire's rolling resistance and cornering performance on soft terrain
(Gheshlaghi et al., 2021)	PAMCRASH	Elastic-plastic hydrodynamic	Soil compaction simulation and validation
(Hu et al., 2022)	CHRONO	Drucker Prager	Traction control of rigid tire on deformable terrain

changes with each time step based on material property defined and undergone deformation. Meanwhile, discrete particle-based methods calculate inter-particle forces to define the overall behavior of the material for given boundary conditions. These formulations allow accurate modeling of discontinuous material undergoing large deformations and separation during failure (Li and Liu, 2002; Bojanowski, 2014; Al-Mahbashi et al., 2020). Application of particle-based methods in soil-tire/tool interaction studies can overcome several limitations of FEM approach. Particle-based methods are not computationally efficient like FEM. However, FEM tends to be computationally more expensive in some cases with large deformations than particle-based methods because of the requirement of frequent remeshing for solution stability (Jayakumar et al., 2017). Some of the particle-based methods employed to study soil tire/tool interaction are discussed in the subsequent sections.

4.4.1. Smoothed particle hydrodynamics

SPH approach is one of the earliest and most matured particle-based methods used to solve computational mechanics problems (Gingold and Monaghan, 1977). SPH was used extensively in solving fluid mechanics and astrophysics problems before it was used in solid mechanics (e.g., geomechanics). In SPH method, the continuum is represented with a set of particles with individual field variables (Fig. 31). The mass and momentum balance equations of continuum are converted to equation of motion which are solved using Lagrangian approach. The field variables like stress, density, and velocity are estimated using an interpolation process in the particle neighborhood. This interpolation process of the field variable is dependent on the smoothing function which determines relative contribution of neighboring particles. The domain of influence of smoothing function is determined by smoothing length (Bui et al., 2008). The interpolation process for a field variable $f(x)$ (Eq. (36))-

$$\langle f(x)\rangle = \int_{\Omega} f(x^{\cdot})W(x-x',h)dx' \tag{36}$$

where, W is smoothing function and h is smoothing length. Solution stability and accuracy are dependent on the smoothing function. Various smoothing functions like gaussian, cubic spline, quadratic and quintic are used in the literature (Monaghan and Lattanzio, 1985; Wendland, 1995; Johnson et al., 1996). Limitations of using SPH method are tensile instability, zero energy mode and modeling of boundary conditions (Li and Liu, 2002).

4.4.1.1. Soil tire interaction studies. SPH method is one of the upcoming methods in the field of terramechanics. As this method is continuum mechanics-based particle method, it is compatible with all the material models used in FEM. This method can model soil penetration and flow under tire with sufficient accuracy unlike FEM which tends to give stiffer responses in such cases. In context of soil-tire interaction, SPH has been used to model soil compaction, steering effort and multipass effect with changing soil moisture content, normal loads, and slip ratios (Table 4) (Dhillon et al., 2013; Gheshlaghi et al., 2021; Surkutwar et al., 2023).

As discussed, SPH method has some inherent stability issues, and it is not yet validated for modeling soil-tire interaction with elastic, elastic–plastic, and elastic-visco-plastic material models. SPH method addresses the limitations of FEM, and it is relatively easy to calibrate compared to DEM. However, before considering this method in general use the stability issues have to be resolved and sufficient validation for all the material models is required with frequently used commercial software like ABAQUS and LS-Dyna (El-Sayegh, 2020).

4.4.1.2. Soil tool interaction studies. In recent soil-tool interaction, SPH methods have been implemented as it is better at capturing soil fragmentation and crack propagation phenomenon occurring during tillage process (Table 5). SPH has inherent stability issues which have been addressed using artificial stress and hourglass control technique for soil-tool interaction studies (Peng et al., 2017). Basic elastic–plastic models are implemented in SPH framework and validated against tool resistance experimental data (Lin

Table 5
Overview of SPH based soil-tool interaction studies.

Author	Software	Soil Material Model	Research Focus
(Major and Csanády, 2014)	ANSYS	Drucker Prager	Cutting forces on rotating soil tiller
(Peng et al., 2017)	–	Von Mises	Soil cutting forces on tillage tool
(Lin et al., 2019)	LS-DYNA	FHWA soil	Soil cutting forces during subsoiling process
(Hu et al., 2023)	User defined Solver	Drucker Prager	Simulation of cutting process in cohesive and non-cohesive soils

et al., 2019). Once validated, SPH approach can be a viable option for modeling cohesive, non-cohesive, strain rate sensitive and unsaturated soils for soil-tool interaction studies (Hu et al., 2023).

4.4.2. Discrete element method

The discrete element method (DEM) is today used extensively in computational modeling of granular material with discontinuous behavior like various types of powder and soils. In DEM, the material is represented with a finite number of particles having different shapes and size. The material behavior is estimated by calculating the inter-particle forces and using equations of motion to track velocity and position of each particle. These inter-particle forces consist of normal and tangential contact forces and distance dependent forces. The normal and tangential contact forces can be calculated using linear or non-linear contact stiffness model along with viscous damping and frictional forces (Fig. 32). Usually, DEM particles can have both translational and rotational DOFs. DEM uses an explicit solving scheme, hence the solution stability is dependent on the time step (Cundall and Strack, 1979; Systemes, 2015).

In most cases, DEM particles are modeled using spherical particles that don't interlock with each other and rotate without dilating. Hence for modeling dilative soils, complex shapes like ellipsoid and poly-ellipsoid are recommended which are computationally more expensive because of its complex contact interaction (Knuth et al., 2012). Some other limitations of implementing DEM are its difficulty in estimating the contact parameter as they cannot be measured through physical experiments and are determined using calibration tools or trail-and-error approach and still large scale models using DEM is not possible because of the requirement of a large number of particles to mimic actual soil behavior which requires high computational time (Horner et al., 2001).

4.4.2.1. Soil tire interaction studies. In terramechanics applications, DEM is used extensively for cohesionless soil as continuum mechanics-based methods have difficulty in modeling soil flow and separation at the tire interface. DEM based soil-tire interaction models are used and validated for predicting soil compaction, drawbar pull and tire sinkage with changing normal load, tread pattern and inflation pressure (Table 6) (Zeng et al., 2020). For these studies, commercial software such as EDEM, Rocky DEM and LS Dyna are used. In addition to that, several researchers have developed in-house DEM codes with focus on soil-tire interaction studies (Wakui and Terumichi, 2011; Zhao and Zang, 2014).

DEM requires 14 parameters in total for definition of soil-soil interaction and soil-tire interaction. Calibration of these parameters and particle size value for simulation is quite difficult as most of them cannot be inferred directly from the soil testing results (Hu et al., 2021). Further, DEM based soil models have limited implementation in modeling unsaturated, cohesive and strain rate sensitive soils for tire interaction studies. Though DEM is validated for modeling cohesion-less soils, still there is a gap in systematic calibration approach and application over wide range of soils in soil-tire interaction studies.

4.4.2.2. Soil tool interaction studies. DEM approach has ability to predict the dynamic nature of soil flow, cracking and mixing of different granular materials essential for modeling soil tool interaction. State of the art review of discrete element method application in soil tool interaction studies provides detail on the contact models, bond models and various calibration techniques used by different researchers (Shmulevich, 2010; Horabik and Molenda, 2016; Aikins et al., 2023). DEM approach based soil-tool interaction studies are used for predicting soil cutting forces and tool wear with changing speed, tool geometry and tillage depth (Table 7). DEM force prediction correlated better with experimental results compared to FEM results which were on the higher side (Ucgul et al., 2018; Tekeste et al., 2019).

Calibration of DEM parameters is usually very difficult especially for cohesive soils where additional cohesion parameters

Table 6
Overview of DEM based soil-tire interaction studies.

Author	Software	Calibration approach	Research Focus
(Hu et al., 2021)	EDEM	Triaxial Test	Drawbar pull and tire steering performance on moist soil
(Wakui and Terumichi, 2011)	User defined Solver	–	Drawbar pull at different slip ratio and cornering performance
(Jayakumar et al., 2017)	DIS/IVRESS	Cone penetrometer test	Influence of soil particle size, particle shape and type on the vehicle mobility
(Nakashima and Takatsu, 2008)	PFC2D	Computational calibration	Tire sinkage and drawbar pull performance
(Zhao and Zang, 2014)	User defined Solver	–	Tire sinkage and drawbar pull performance
(Xu et al., 2020)	LS-DYNA	Triaxial Test	Sinkage and traction performance of tire on gravel road
(Zeng et al., 2020)	LS-DYNA	Triaxial Test	Influence of tread pattern, and slip ratio on tractive performance
(Smith and Peng, 2013)	LIGGGHTS	–	Sinkage, drawbar pull and driving torque estimation
(Zang and Zhao, 2013)	User defined Solver	–	Sinkage and drawbar pull performance
(Castañeda et al., 2021)	Rocky DEM	–	Drawbar pull performance on deformable terrain
(Oida and Momozu, 2002)	User defined Solver	–	Effect of lug geometry on tire tractive performance on deformable terrain
(Nakashima et al., 2010)	PFC2D	Computational calibration	Rigid wheel performance on inclined slope of Lunar simulant
(Du et al., 2017)	PFC3D	Triaxial Test	Effect of lug geometry on tire steering tractive parameters on sand

Table 7
Overview of DEM based soil-tool interaction studies.

Author	Software	Calibration approach	Research Focus
(Sadek et al., 2021)	PFC 3D	Computational calibration	Draft force of disc implement
(Makange et al., 2020)	EDEM	Angle of repose test	Soil failure pattern and cutting forces
(Qi et al., 2019)	PFC 3D	Angle of repose test	Soil flow and effect of particle size on simulation results
(Kim et al., 2021)	EDEM	Field measurement	Draft force prediction for plough in cohesive soil
(Saunders et al., 2021)	EDEM	Computational calibration	Draft force of skimmer at different speed and depth
(Tekeste et al., 2020)	EDEM	Computational calibration	Soil forces at soil-bulldozer blade interface
(Tekeste et al., 2019)	EDEM	Computational calibration	Cultivator sweep tool wearing effect on soil draft forces and soil flow pattern
(Ucgul et al., 2018)	EDEM	Computational calibration	Tillage forces and soil flow pattern

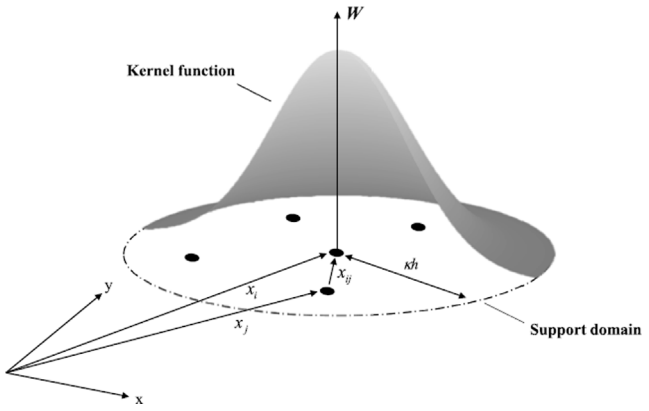

Fig. 31. Interpolation of field variables in SPH method. Redrawn from (Seo et al., 2021).

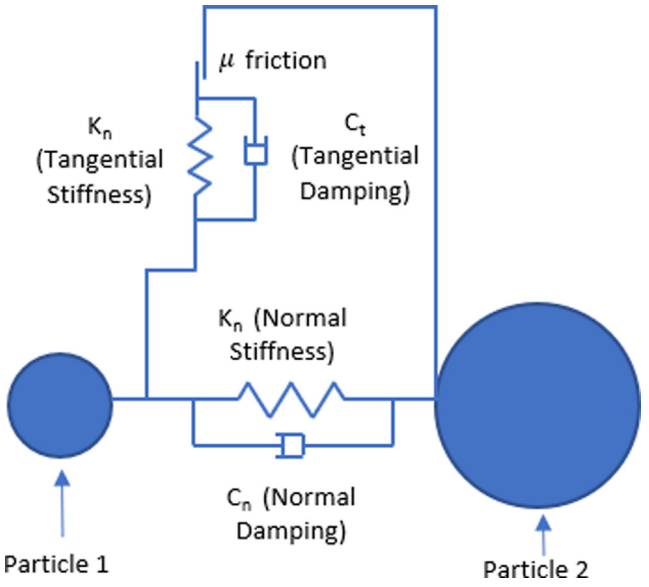

Fig. 32. Normal and Tangential contact interaction in DEM method. Redrawn from (Systemes, 2015).

are also required for the modeling realistic behavior of soil. Unlike FEM, DEM parameters cannot be calibrated easily using in-situ test results and requires extensive soil laboratory testing data. Validation of DEM in terms of soil flow and soil displacement is not simple, as for the correlation of simulation and experimental results the DEM particle size has to be close to the actual particle size of soil, which increases the simulation time by a considerable amount. Further, effect of initial void ratio, particle shape and size, particle breakage, particle distribution, contact formulation of cohesive soils and moisture content on soil-tool interaction studies has to be analyzed (Jafari et al., 2006; Al-Kheer et al., 2011). In addition to commercial software, terramechanics-focused open source code CHRONO can also be used (Tasora et al., 2016).

5. Summary

Identification of soil physical and mechanical properties is quite complex. Tire and agricultural tools performance on any soil is highly dependent on the shear strength of the soil which significantly varies with moisture content, loading conditions, strain rate and stress history. Failure envelope of the soil can be obtained using laboratory tests like direct shear test and triaxial test. It can also be estimated using in-situ testing like cone penetrometer, but it is heavily dependent on the empirical relations which can be used only to determine the parameters in dry and saturated conditions. For unsaturated soil characterization, no generalized empirical relations exist. In continuum mechanics-based framework, elastic, elastic–plastic and elastic-viscoplastic constitutive models are used in soil-tire/tool interaction studies. Empirical and analytical models used in soil-tire/tool interactions in the past are simple to implement using field testing data, but they only provide limited information. Finite element and particle-based numerical methods are preferred to conduct detailed study of soil-tire/tool interaction. FE methods with various meshing algorithms are used out of which ALE approach correlates better with the real behavior of the soil. FE methods still are not suitable for modeling of large deformation and discontinuous behavior of the soil. Particle-based methods based on continuum (SPH) and discrete (DEM) approach which overcomes the limitations of FE methods are also used in soil-tire/tool interaction modeling. These particle-based methods, though moderately mature, need to be evaluated in more depth and improved for these specific applications.

Declaration of Competing Interest

The authors declare that they have no known competing financial interests or personal relationships that could have appeared to influence the work reported in this paper.

Acknowledgments

This study has been partially supported by the Center for Tire Research (CenTiRe), an NSF-I/UCRC (Industry/University Cooperative Research Center) at Virginia Tech and by the Center for Injury Biomechanics (CIB) at Virginia Tech. The authors wish to thank the project mentors and the members of the industrial advisory board of CenTiRe for their support and guidance.

References

Abo-Elnor, M. et al., 2004. Simulation of soil–blade interaction for sandy soil using advanced 3D finite element analysis. Soil Tillage Res. 75 (1), 61–73.
Abu-Hamdeh, N.H., Reeder, R.C., 2003. Measuring and predicting stress distribution under tractive devices in undisturbed soils. Biosyst. Eng. 85 (4), 493–502.
Adams, B., 2002. Elastoplastic soil mechanics. Advances in Soil Dynamics, vol. 2. American Society of Agricultural and Biological Engineers, p. 1.
Aikins, K.A. et al., 2023. Review of discrete element method simulations of soil tillage and furrow opening. Agriculture 13 (3), 541.
Alavi, N., Hojati, R., 2012. Modeling the soil cutting process in rotary tillers using finite element method. J. Agric. Technol. 8 (1), 27–37.
Al-Kheer, A.A. et al., 2011. Estimating the variability of tillage forces on a chisel plough shank by modeling the variability of tillage system parameters. Comput. Electron. Agric. 78 (1), 61–70.
Al-Mahbashi, A.M. et al., 2020. Soil–water characteristic curve and one-dimensional deformation characteristics of fiber-reinforced lime-blended expansive soil. J. Mater. Civ. Eng. 32 (6), 04020125.
Alonso, E.E. et al., 1990. A constitutive model for partially saturated soils. Geotechnique 40 (3), 405–430.
Armin, A. et al., 2017. Experimental and finite element analysis for mechanics of soil-tool interaction. Int. J. Mech. Mechatron. Eng. 11 (2), 433–439.
Atkinson, J., 2000. Non-linear soil stiffness in routine design. Geotechnique 50 (5), 487–508.
Aversa, S., Nicotera, M.V., 2002. A triaxial and oedometer apparatus for testing unsaturated soils. Geotech. Test. J. 25 (1), 3–15.
Banerjee, A., 2017. Response of unsaturated soils under monotonic and dynamic loading over moderate suction states.
Bekakos, C.-A. et al., 2017. Finite element modelling of a pneumatic tyre interacting with rigid road and deformable terrain. Int. J. Vehicle Performance 3 (2), 142–166.
Bekakos, C., et al., 2015. Dynamic response of rigid wheels on deformable terrains.
Bekker, M.G., 1956. Theory of land locomotion.
Benz, T. et al., 2008. A Lode angle dependent formulation of the hardening soil model. The 12th International Conference of International Association for Computer Methods and Advances in Geomechanics (IACMAG).

Bigoni, D., Zaccaria, D., 1992. Loss of strong ellipticity in non-associative elastoplasticity. J. Mech. Phys. Solids 40 (6), 1313–1331.
Bishop, A.W., 1959. The principle of effective stress. Teknisk ukeblad 39, 859–863.
Bojanowski, C., 2014. Numerical modeling of large deformations in soil structure interaction problems using FE, EFG, SPH, and MM-ALE formulations. Arch. Appl. Mech. 84 (5), 743–755.
Boman, R., Ponthot, J.-P., 2004. Finite element simulation of lubricated contact in rolling using the arbitrary Lagrangian-Eulerian formulation. Comput. Methods Appl. Mech. Eng. 193 (39–41), 4323–4353.
Brinkgreve, R.B., 2005. Selection of soil models and parameters for geotechnical engineering application. Soil Constitutive Models: Eval. Select. Calibrat., 69–98
Brinkgreve, R., et al., 2016. PLAXIS 2016. PLAXIS bv, the Netherlands.
Budhu, M., 2015. Soil Mechanics Fundamentals. John Wiley & Sons.
Bui, H.H. et al., 2008. Lagrangian meshfree particles method (SPH) for large deformation and failure flows of geomaterial using elastic–plastic soil constitutive model. Int. J. Numer. Anal. Meth. Geomech. 32 (12), 1537–1570.
Casagrande, A., 1936. The determination of pre-consolidation load and it's practical significance. In: Proc. Int. Conf. Soil Mech. Found. Eng. Cambridge, Mass., p. 1936.
Castañeda, E.A. et al., 2021. FEM and DEM simulations of tire-soil and drill-soil interactions in off-road conditions for mechanical design validation of a space exploration rover. 2021 12th International Conference on Mechanical and Aerospace Engineering (ICMAE). IEEE.
Chauhan, P. et al., 2019. Unsaturated behavior of rammed earth: Experimentation towards numerical modelling. Constr. Build. Mater. 227, 116646.
Chen, W.-F., 2007. Plasticity in Reinforced Concrete. J. Ross Publishing.
Chi, L., Kushwaha, R., 1990. A non-linear 3-D finite element analysis of soil failure with tillage tools. J. Terramech. 27 (4), 343–366.
Chiroux, R.C., et al., 2005. Three-dimensional finite element analysis of soil interaction with a rigid wheel.
Contreras, U. et al., 2013. Soil models and vehicle system dynamics. Appl. Mech. Rev. 65 (4).
Coulomb, C., 1776. Essai sur une application des regles de Maximums et Minimis á quelques.
Cueto, O.G. et al., 2013. Three dimensional finite element model of soil compaction caused by agricultural tire traffic. Comput. Electron. Agric. 99, 146–152.
Cundall, P.A., Strack, O.D., 1979. A discrete numerical model for granular assemblies. Geotechnique 29 (1), 47–65.
Das, B.M., 2021. Principles of Geotechnical Engineering. Cengage learning.
Day, R., 2001. Soil testing manual: procedures. Classif.Data Sampling Practices.
De Borst, R. et al., 2012. Nonlinear Finite Element Analysis of Solids and Structures. John Wiley & Sons.
De Borst, R., 1986. Non-linear analysis of frictional materials.
De'an, S. et al., 2000. An elasto-plastic model for unsaturated soil in three-dimensional stresses. Soils Found. 40 (3), 17–28.
Dechao, Z., Yusu, Y., 1992. A dynamic model for soil cutting by blade and tine. J. Terramech. 29 (3), 317–327.
Deng, Y.-J. et al., 2019. Finite element modeling of interaction between non-pneumatic mechanical elastic wheel and soil. Proc. Inst. Mech. Eng., Part D: J. Automobile Eng. 233 (13), 3293–3304.
Dhillon, R.S., et al., 2013. Development of truck tire-soil interaction model using FEA and SPH, SAE Technical Paper.
DiMaggio, F.L., Sandler, I.S., 1971. Material model for granular soils. J .Eng. Mech. Div. 97 (3), 935–950.
Ding, L. et al., 2014. New perspective on characterizing pressure–sinkage relationship of terrains for estimating interaction mechanics. J. Terramech. 52, 57–76.
Drucker, D. et al., 1952. Extended limit design theorems for continuous media. Q. Appl. Math. 9 (4), 381–389.
Drucker, D.C. et al., 1957. Soil mechanics and work-hardening theories of plasticity. Trans. Am. Soc. Civ. Eng. 122 (1), 338–346.
Drumright, E.E., 1989. The Contribution of Matric Suction to the Shear Strength of Unsaturated Soils. Colorado State University.
Du, X. et al., 2017a. Numerical analysis of the dynamic interaction between a non-pneumatic mechanical elastic wheel and soil containing an obstacle. Proc. Inst. Mech. Eng., Part D: J. Automobile Eng. 231 (6), 731–742.
Du, Y. et al., 2017b. Numerical analysis on tractive performance of off-road wheel steering on sand using discrete element method. J. Terramech. 71, 25–43.
Duncan, J.M., Chang, C.-Y., 1970. Nonlinear analysis of stress and strain in soils. J. Soil Mech. Found. Division 96 (5), 1629–1653.
El-Gindy, M., et al., 2011. Soil modeling using FEA and SPH techniques for a tire-soil interaction. In: International Design Engineering Technical Conferences and Computers and Information in Engineering Conference.
El-Sayegh, Z. et al., 2018. Improved tire-soil interaction model using FEA-SPH simulation. J. Terramech. 78, 53–62.
El-Sayegh, Z., 2020. Modeling and analysis of truck tire-terrain interaction. University of Ontario Institute of Technology.
Escario, V., Saez, J., 1987. Shear strength of partly saturated soils versus suction. In: Proceedings of the International Conference on Expansive Soils.
Eslami, A., S. Moshfeghi, H. Molaabasi and M. M. Eslami (2019). Piezocone and cone penetration test (CPTu and CPT) applications in foundation engineering, Butterworth-Heinemann.
Eyo, E.U. et al., 2020. An overview of soil–water characteristic curves of stabilised soils and their influential factors. J. King Saud Univ.-Eng Sci.
Farhadi, P. et al., 2019. Finite element modeling of the interaction of a treaded tire with clay-loam soil. Comput. Electron. Agric. 162, 793–806.
Fervers, C., 2004. Improved FEM simulation model for tire–soil interaction. J. Terramech. 41 (2–3), 87–100.
Fielke, J.M., 1999. Finite element modelling of the interaction of the cutting edge of tillage implements with soil. J. Agric. Eng. Res. 74 (1), 91–101.
Fredlund, D.G., et al., 1987. Non-linearity of strength envelope for unsaturated soils. In: Proceedings of the 6th International Conference on Expansive Soils, New Delhi, India.
Fredlund, D.G., Morgenstern, N., 1976. Constitutive relations for volume change in unsaturated soils. Can. Geotech. J. 13 (3), 261–276.
Fredlund, D.G., Morgenstern, N.R., 1977. Stress state variables for unsaturated soils. J. Geotech. Eng. Div. 103 (5), 447–466.
Fredlund, D.G., Rahardjo, H., 1993. Soil Mechanics for Unsaturated Soils. John Wiley & Sons.
Gan, J. et al., 1988. Determination of the shear strength parameters of an unsaturated soil using the direct shear test. Can. Geotech. J. 25 (3), 500–510.
Gee-Clough, D., 1976. The Bekker theory of rolling resistance amended to take account of skid and deep sinkage. J. Terramech. 13 (2), 87–105.
Gheshlaghi, F. et al., 2021b. Investigating the effects of off-road vehicles on soil compaction using FEA-SPH simulation. Int. J. Heavy Veh. Syst. 28 (3), 455–466.
Gheshlaghi, F., et al., 2021. Advanced analytical truck tires-terrain interaction model, SAE Technical Paper.
Gingold, R.A., Monaghan, J.J., 1977. Smoothed particle hydrodynamics: theory and application to non-spherical stars. MNRAS 181 (3), 375–389.
Głuchowski, A. et al., 2020. Laboratory characterization of a compacted–unsaturated silty sand with special attention to dynamic behavior. Appl. Sci. 10 (7), 2559.
Hambleton, J.P., 2010. Plastic Analysis of Processes Involving Material-Object Interaction. University of Minnesota.
Hambleton, J., Drescher, A., 2009. On modeling a rolling wheel in the presence of plastic deformation as a three-or two-dimensional process. Int. J. Mech. Sci. 51 (11–12), 846–855.
Han, Z., Vanapalli, S., 2016. Stiffness and shear strength of unsaturated soils in relation to soil-water characteristic curve. Geotechnique 66 (8), 627–647.
He, R. et al., 2019. Review of terramechanics models and their applicability to real-time applications. J. Terramech. 81, 3–22.
He, R., 2020. Systematic Tire Testing and Model Parameterization for Tire Traction on Soft Soil, Virginia Tech.
Helwany, S., 2007. Applied Soil Mechanics with ABAQUS Applications. John Wiley & Sons.
Hettiaratchi, D., Reece, A., 1967. Symmetrical three-dimensional soil failure. J. Terramech. 4 (3), 45–67.
Hibbitt, H. et al., 2013. ABAQUS Version 6.13: CAE User's Manual, Analysis User's manual, Example Problems Manual, Keyword Reference Manual, Theory Manual, User Subroutines Reference Manual. HKS Inc, Rhode Island.
Ho, D. et al., 1992. Volume change indices during loading and unloading of an unsaturated soil. Can. Geotech. J. 29 (2), 195–207.
Horabik, J., Molenda, M., 2016. Parameters and contact models for DEM simulations of agricultural granular materials: A review. Biosyst. Eng. 147, 206–225.
Horner, D.A. et al., 2001. Large scale discrete element modeling of vehicle-soil interaction. J. Eng. Mech. 127 (10), 1027–1032.
Hu, C. et al., 2021. Numerical simulation of tire steering on sandy soil based on discrete element method. AIP Adv. 11, (1) 015015.
Hu, W. et al., 2022. Traction control design for off-road mobility using an SPH-DAE cosimulation framework. Multibody Sys.Dyn. 55 (1–2), 165–188.
Hu, M. et al., 2023. Simulation of soil-tool interaction using smoothed particle hydrodynamics (SPH). Soil Tillage Res. 229, 105671.
Huang, F. et al., 2022. A Study on the Shear Strength Characteristic of Unsaturated Red Clay. World J. Eng. Technol. 10 (4), 714–727.
Huat, B. et al., 2005. Modified shear box test apparatus for measuring shear strength of unsaturated residual soil. Am. J. Appl. Sci. 2 (9), 1283–1289.
Jafari, R., et al., 2006. Large deformation modeling in soil-tillage tool interaction using advanced 3D nonlinear finite element approach. In: Proceedings of the 6th WSEAS International Conference on Simulation, Modelling and Optimization.
Janosi, Z., Command, O.T.-A., 1959. Prediction of'' WES Cone Index" by Means of a Stress-strain Function of Soils, Ordnance Tank-Automotive Command.
Janosi, Z,. Hanamoto, B., 1961. An analysis of the drawbar pull vs slip relationship for track laying vehicles, Army Tank-Automotive Center Warren MI.
Jarast, P., Ghayoomi, M., 2018. Numerical modeling of cone penetration test in unsaturated sand inside a calibration chamber. Int. J. Geomech. 18 (2), 04017148.
Jayakumar, P. et al., 2017. Understanding the effects of soil characteristics on mobility. International Design Engineering Technical Conferences and Computers and Information in Engineering Conference. American Society of Mechanical Engineers.
Jefferies, M.G., Shuttle, D.A., 2005. NorSand: features, calibration and use. Soil constitutive models: evaluation, selection, and calibration: 204–236.
Jiang, H., Xie, Y., 2011. A note on the Mohr-Coulomb and Drucker-Prager strength criteria. Mech. Res. Commun. 38 (4), 309–314.
Johnson, G.R. et al., 1996. SPH for high velocity impact computations. Comput. Methods Appl. Mech. Eng. 139 (1–4), 347–373.

Karafiath, L.L., Sobierajsku, F.S., 1974. Effect of Speed on Tire-Soil Interaction and Development of Towed Pneumatic Tire-Soil Model, Grumman Aerospace Corp Bethpage NY Research DEPT.
Karmakar, S. et al., 2009. Experimental validation of computational fluid dynamics modeling for narrow tillage tool draft. J. Terramech. 46 (6), 277–283.
Keaton, J.R., 2018. Noncohesive Soils. In: Bobrowsky, P.T., Marker, B. (Eds.), Encyclopedia of Engineering Geology. Springer International Publishing, Cham, pp. 689–690.
Khalili, N. et al., 2004. Effective stress in unsaturated soils: Review with new evidence. Int. J. Geomech. 4 (2), 115–126.
Khalili, N., Khabbaz, M., 1998. A unique relationship for χ for the determination of the shear strength of unsaturated soils. Geotechnique 48 (5), 681–687.
Kim, Y.-S. et al., 2021. DEM simulation for draft force prediction of moldboard plow according to the tillage depth in cohesive soil. Comput. Electron. Agric. 189, 106368.
Kim, M.K., Lade, P.V., 1988. Single hardening constitutive model for frictional materials: I. Plastic potential function. Comput. Geotech. 5 (4), 307–324.
Knuth, M.A. et al., 2012. Discrete element modeling of a Mars Exploration Rover wheel in granular material. J. Terramech. 49 (1), 27–36.
Kohgo, Y. et al., 1993. Theoretical aspects of constitutive modelling for unsaturated soils. Soils Found. 33 (4), 49–63.
Kondner, R.L., 1963. Hyperbolic stress-strain response: cohesive soils. J. Soil Mech. Found. Divis. 89 (1), 115–143.
Kushwaha, R. et al., 1993. Analytical and numerical models for predicting soil forces on narrow tillage tools. Can. Agric. Eng. 35 (3), 183.
Kushwaha, R., Shen, J., 1995. Finite element analysis of the dynamic interaction between soil and tillage tool. Trans. ASAE 38 (5), 1315–1319.
Lade, P.V., 2016. Triaxial Testing of Soils. John Wiley & Sons.
Li, M. et al., 2015. A 3D finite element simulation analysis of the soil forces acting on a rotary blade. Trans. ASABE 58 (2), 243–249.
Li, S., Liu, W.K., 2002. Meshfree and particle methods and their applications. Appl. Mech. Rev. 55 (1), 1–34.
Li, H., Schindler, C., 2013. Analysis of soil compaction and tire mobility with finite element method. Proc. Inst. Mech. Eng., Part K: J. Multi-body Dyn. 227 (3), 275–291.
Likitlersuang, S., Teachavorasinskun, S., Surarak, C., Oh, E., Balasubramaniam, A., 2013. Small strain stiffness and stiffness degradation curve of Bangkok Clays. Soils and foundations 53 (4), 498–509.
Lin, Y. et al., 2019. Virtual simulation technology based research on subsoiling process. Proc. Inst. Mech. Eng. C J. Mech. Eng. Sci. 233 (5), 1493–1503.
Lings, M., Dietz, M., 2005. The peak strength of sand-steel interfaces and the role of dilation. Soils Found. 45 (6), 1–14.
Liu, C., Wong, J., 1996. Numerical simulations of tire-soil interaction based on critical state soil mechanics. J. Terramech. 33 (5), 209–221.
Ma, J., et al., 2009. Numerical Simulation of New Generation Non-Pneumatic Tire (TWEEL™) and Sand. In: International Design Engineering Technical Conferences and Computers and Information in Engineering Conference.
Major, T., Csanády, V., 2014. Application of numerical analysis for the design of rotating tools. Hungarian Agric. Eng. 26, 16–19.
Makange, N.R. et al., 2020. Prediction of cutting forces and soil behavior with discrete element simulation. Comput. Electron. Agric. 179, 105848.
Mitchell, J. K., et al., 1978. Measurement of soil properties in-situ. Present methods: their applicability and potential, California Univ., Berkeley (USA). Lawrence Berkeley Lab.
Mohr, O. 1900. Welche umstände bedingen die elastizitätsgrenze und den bruch eines materials? z ver deut ing. Quoted on: 6.
Monaghan, J.J., Lattanzio, J.C., 1985. A refined particle method for astrophysical problems. A & A 149, 135–143.
Mouazen, A.M., Neményi, M., 1999. Finite element analysis of subsoiler cutting in non-homogeneous sandy loam soil. Soil Tillage Res. 51 (1–2), 1–15.
Mulqueen, J. et al., 1977. Evaluation of penetrometers for measuring soil strength. J. Terramech. 14 (3), 137–151.
Muro, T., O'Brien, J., 2004. Terramechanics: Land Locomotion Mechanics. CRC Press.
Nakashima, H. et al., 2010. Discrete element method analysis of single wheel performance for a small lunar rover on sloped terrain. J. Terramech. 47 (5), 307–321.
Nakashima, H., Takatsu, Y., 2008. Analysis of tire tractive performance on deformable terrain by finite element-discrete element method. J. Comput. Sci. Technol 2 (4), 423–434.
Nam, S. et al., 2011. Determination of the shear strength of unsaturated soils using the multistage direct shear test. Eng. Geol. 122 (3–4), 272–280.
Naylor, D.J., et al., 1981. Finite elements in geotechnical engineering. Pineridge Press Ltd. Swansea, U. K.(SW/75), 1981, 245.
Nayyeri Amiri, S., 2010. A Comprehensive Study on Soil Consolidation. Kansas State University.
Ng, C.W.W. et al., 2009. Effects of wetting–drying and stress ratio on anisotropic stiffness of an unsaturated soil at very small strains. Can. Geotech. J. 46 (9), 1062–1076.
NRCS, U., 1993. Soil survey division staff (1993) soil survey manual. Soil conservation service. US Department of Agriculture Handbook 18, 315.
Öberg, A., Sällfors, G., 1997. Determination of shear strength parameters of unsaturated silts and sands based on the water retention curve. Geotech. Test. J. 20 (1), 40–48.
Obermayr, M., Öngün, Y., 2010. Simulation of soil-machine interaction in agricultural engineering. Dreßler.
Oh, W.T. et al., 2009. Semi-empirical model for the prediction of modulus of elasticity for unsaturated soils. Can. Geotech. J. 46 (8), 903–914.
Oida, S. et al., 2005. Soil/tire interaction analysis using FEM and FVM. Tire Sci. Technol. 33 (1), 38–62.
Oida, A., Momozu, M., 2002. Simulation of soil behavior and reaction by machine part by means of DEM. Agric. Eng. Int.: CIGR J.
Papamichael, S., 2019. Experimental and numerical investigations on wheel-soil interactions in calibrated near-surface soil model, Technische Universität Kaiserslautern.
Payne, P., 1956. The relationship between the mechanical properties of soil and the performance of simple cultivation implements. J. Agric. Eng. Res. 1 (1), 23–50.
Peng, C., et al., 2017. Large deformation modeling of soil-machine interaction in clay. Bifurcation and Degradation of Geomaterials with Engineering Applications: Proceedings of the 11th International Workshop on Bifurcation and Degradation in Geomaterials dedicated to Hans Muhlhaus, Limassol, Cyprus, 21-25 May 2017 11, Springer.
Perzyna, P., 1966. Fundamental problems in viscoplasticity. Adv. Appl. Mech. 9, 243–377.
Poodt, M. et al., 2003. FEM analysis of subsoil reaction on heavy wheel loads with emphasis on soil preconsolidation stress and cohesion. Soil Tillage Res. 73 (1–2), 67–76.
Potts, D.M. et al., 2001. Finite Element Analysis in Geotechnical Engineering: Application. Thomas Telford London.
Pournaghiazar, M. et al., 2013. The cone penetration test in unsaturated sands. Geotechnique 63 (14), 1209–1220.
Prajapati, V., Das, A., 2023. Numerical implementation of BBM in FE package for solving unsaturated soil boundary value problems. E3S Web of Conferences, EDP Sciences.
Prevost, J.H., Popescu, R., 1996. Constitutive relations for soil materials. Electron. J. Geotech. Eng. 1, 1–45.
Puzrin, A., 2012. Constitutive Modelling in Geomechanics: Introduction. Springer Science & Business Media.
Qi, L. et al., 2019. Simulations of soil flow properties using the discrete element method (DEM). Comput. Electron. Agric. 157, 254–260.
Ragheb, H., et al., 2013. Development of a combat vehicle fea tire model for off-road applications. SAE 2013 World Congress & Exhibition.
Reece, A.R., 1965. Principles of soil-vehicle mechanics. Proc. Inst. Mech. Eng.: Automobile Divis. 180 (1), 45–66.
Rohani, B., Baladi, G.Y., 1981. Correlation of mobility cone index with fundamental engineering properties of soil.
Roscoe, K. et al., 1963. Yielding of clays in states wetter than critical. Geotechnique 13 (3), 211–240.
Roscoe, K.H., Burland, J., 1968. On the generalized stress-strain behaviour of wet clay.
Rula, A.A., Nuttall, Jr. C.J., 1971. An analysis of ground mobility models (ANAMOB), Army Engineer Waterways Experiment Station Vicksburg Ms.
Russell, A., Khalili, N., 2006. A unified bounding surface plasticity model for unsaturated soils. Int. J. Numer. Anal. Meth. Geomech. 30 (3), 181–212.
Sadek, M.A. et al., 2021. Draft force prediction for a high-speed disc implement using discrete element modelling. Biosyst. Eng. 202, 133–141.
Saliba, J.E., 1990. Elastic-viscoplastic finite-element program for modeling tire/soil interaction. J. Aircr. 27 (4), 350–357.
Saunders, C. et al., 2021. Discrete element method (DEM) simulation to improve performance of a mouldboard skimmer. Soil Tillage Res. 205, 104764.
Sawangsuriya, A. et al., 2009. Modulus-suction-moisture relationship for compacted soils in postcompaction state. J. Geotech. Geoenviron. Eng. 135 (10), 1390.
Schanz, T., et al., 2010. Bearing capacity of a strip footing on an unsaturated sand. Unsaturated Soils, Two Volume Set, CRC Press, pp. 1195–1200.
Schofield, A.N., Wroth, P., 1968. Critical State Soil Mechanics. McGraw-hill London.
Scott, R.F., 1985. Plasticity and constitutive relations in soil mechanics. J. Geotech. Eng. 111 (5), 559–605.
Seo, H.-D., Park, H.-J., Kim, J.-I., Lee, P.S., 2021. The particle-attached element interpolation for density correction in smoothed particle hydrodynamics. Advances in Engineering Software 154, 102972.
Shmulevich, I., 2010. State of the art modeling of soil–tillage interaction using discrete element method. Soil Tillage Res. 111 (1), 41–53.
Shoop, S., et al., 2005. Constitutive model for a thawing, frost-susceptible sand, Engineer Research And Development Center Hanover NH Cold Regions Research. . ..
Slatter, E.E., et al., 2000. Suction controlled testing of unsaturated soils with an osmotic oedometer. ISRM International Symposium, OnePetro.
Smed, E., Cundall, P., 2012. Elasto-plasto Strain Hardening Mohr-Coulomb Model-Derivation and Implementation, Aalborg, Denmark.
Smith, W., Peng, H., 2013. Modeling of wheel–soil interaction over rough terrain using the discrete element method. J. Terramech. 50 (5–6), 277–287.
Souli, M., Shahrour, I., 2012. Arbitrary Lagrangian Eulerian formulation for soil structure interaction problems. Soil Dyn. Earthq. Eng. 35, 72–79.
Stoltz, G. et al., 2012. Multi-scale analysis of the swelling and shrinkage of a lime-treated expansive clayey soil. Appl. Clay Sci. 61, 44–51.
Sumelka, W., 2014. A note on non-associated Drucker-Prager plastic flow in terms of fractional calculus. J. Theor. Appl. Mech. 52 (2), 571–574.
Surkutwar, Y., C. Sandu and C. Untaroiu (2023). "Review of modeling methods of compressed snow-tire interaction." Journal of terramechanics 105: 27-40.

Swamy, V. S., R. Pandit, A. Yerro, C. Sandu, D. M. Rizzo, K. Sebeck and D. Gorsich (2023). "Review of modeling and validation techniques for tire-deformable soil interactions." Journal of terramechanics 109: 73-92.
Swick, W., Perumpral, J., 1988. A model for predicting soil-tool interaction. J. Terramech. 25 (1), 43–56.
Systemes, D., 2015. Abaqus 6.14 documentation–theory guide. Providence, RI.
Tagar, A. et al., 2015. Finite element simulation of soil failure patterns under soil bin and field testing conditions. Soil Tillage Res. 145, 157–170.
Tasora, A., et al., 2016. Chrono: An open source multi-physics dynamics engine. High Performance Computing in Science and Engineering: Second International Conference, HPCSE 2015, Soláň, Czech Republic, May 25-28, 2015, Revised Selected Papers 2, Springer.
Tekeste, M.Z. et al., 2019. Discrete element modeling of cultivator sweep-to-soil interaction: Worn and hardened edges effects on soil-tool forces and soil flow. J. Terramech. 82, 1–11.
Tekeste, M.Z. et al., 2020. Modeling soil-bulldozer blade interaction using the discrete element method (DEM). J. Terramech. 88, 41–52.
Terzaghi, K., 1943. Theoretical Soil Mechanics. John Wiley Sons.
Terzaghi, K., Peck, R.B., 1948. Soil Mechanics. Engineering Practice. John Wiley and Sons, Inc., New York.
Toll, D., 1990. A framework for unsaturated soil behaviour. Geotechnique 40 (1), 31–44.
Toll, D., Ong, B., 2003. Critical-state parameters for an unsaturated residual sandy clay. Geotechnique 53 (1), 93–103.
Trower, M., Emerson, J., Yu, M., Vivacqua, V., Johnson, T., Stitt, H., Dos Reis, G., 2023. Reduced-order hybrid modelling for powder compaction: predicting density and classifying diametrical hardness. Powder Technology, 118745.
Ucgul, M. et al., 2018. Comparison of the discrete element and finite element methods to model the interaction of soil and tool cutting edge. Biosyst. Eng. 169, 199–208.
Vanapalli, S. et al., 1996. Model for the prediction of shear strength with respect to soil suction. Can. Geotech. J. 33 (3), 379–392.
Vanapalli, S., 2009. Shear strength of unsaturated soils and its applications in geotechnical engineering practice. Keynote Address. Proc. 4th Asia-Pacific Conf. on Unsaturated Soils. New Castle, Australia.
Wakui, F., Terumichi, Y., 2011. Numerical simulation of tire behavior on soft ground. J. Syst. Des. Dyn. 5 (3), 486–500.
Wang, Y. et al., 2015. Effects of aggregate size on water retention capacity and microstructure of lime-treated silty soil. Géotech. Lett. 5 (4), 269–274.
Wang, H. et al., 2017. Application of terramechanics in off-road vehicle performance prediction. Proceedings 5th International Conference on Mechanics and Mechatronics (ICMM).
Wen, H. et al., 2015. Soil–water characteristic curves for soils stabilized with class C fly ash. Transp. Res. Rec. 2473 (1), 147–154.
Wendland, H., 1995. Piecewise polynomial, positive definite and compactly supported radial functions of minimal degree. Adv. Comput. Mathe. 4 (1), 389–396.
Wong, J. et al., 1984. Theoretical prediction and experimental substantiation of the ground pressure distribution and tractive performance of tracked vehicles. Proc. Inst. Mech. Eng., Part D: Transport Eng. 198 (4), 265–285.
Wong, J.Y., 1989. Terramechanics and Off-road Vehicles. Elsevier.
Wong, J.Y., 2022. Theory of Ground Vehicles. John Wiley & Sons.
Wright, A., 2012. Tyre/soil interaction modelling within a virtual proving ground environment.
Wulfsohn, D. et al., 1998. Triaxial testing of unsaturated agricultural soils. J. Agric. Eng. Res. 69 (4), 317–330.
Xia, K., 2011. Finite element modeling of tire/terrain interaction: Application to predicting soil compaction and tire mobility. J. Terramech. 48 (2), 113–123.
Xiang, X., Zi-Hang, D., 2017. Numerical implementation of a modified Mohr-Coulomb model and its application in slope stability analysis. J. Modern Transport. 25 (1), 40–51.
Xu, W. et al., 2020. Numerical analysis on tractive performance of off-road tire on gravel road using a calibrated finite element method–discrete element method model and experimental validation. Proc. Inst. Mech. Eng., Part D: J. Automobile Eng. 234 (14), 3440–3457.
Yamashita, H. et al., 2018. Physics-based deformable tire–soil interaction model for off-road mobility simulation and experimental validation. J. Comput. Nonlinear Dyn. 13 (2).
Yu, H.-S., 1998. CASM: A unified state parameter model for clay and sand. Int. J. Numer. Anal. Meth. Geomech. 22 (8), 621–653.
Zang, M., Zhao, C., 2013. Numerical simulation of rigid wheel running behavior on sand terrain. APCOM & ISCM 21, 43.
Zeng, H. et al., 2020. Experimental and numerical investigations of tractive performance of off-road tires on gravel terrain. Int. J. Comput. Methods 17 (08), 1950055.
Zhang, L. et al., 2018. A novel approach for simulation of soil-tool interaction based on an arbitrary Lagrangian-Eulerian description. Soil Tillage Res. 178, 41–49.
Zhao, C., Zang, M., 2014. Analysis of rigid tire traction performance on a sandy soil by 3D finite element–discrete element method. J. Terramech. 55, 29–37.
Zhu, L. et al., 2017. Modeling of share/soil interaction of a horizontally reversible plow using computational fluid dynamics. J. Terramech. 72, 1–8.